DYNAMIC STRESS FROM TRANSVERSE IMPACT ON FLEXURAL BEAMS

by

JOSHUA BALLARD

Presented to the Faculty of the Graduate School of

The University of Texas at Arlington in Partial Fulfillment

of the Requirements

for the Degree of

MASTER OF SCIENCE IN MECHANICAL ENGINEERING

THE UNIVERSITY OF TEXAS AT ARLINGTON

December 2009

ACKNOWLEDGEMENTS

I would like to thank a few people for their support and guidance. Brady Richard at Environmental Testing Laboratory gave me use of his data acquisition hardware and software. Dr. Louis Bellott helped with the initial concept for the project and assisted in some of the mechanical aspects of the testing. Aditya Battin performed the finite element analysis, for which I am very thankful. Dr. Kent Lawrence gave insight and support as my thesis advisor. I would also like to thank Dr. Chan and Dr. Wang for being on my committee.

November 25, 2009

ABSTRACT

DYNAMIC STRESS FROM TRANSVERSE

IMPACT ON FLEXURAL BEAMS

Joshua Ballard, M.S.

The University of Texas at Arlington, 2009

Supervising Professor: Kent Lawrence

Accurate prediction of stress from impact would be very useful to an engineer in the design and analysis phases of a project. Currently one must resort to finite element analysis and experimentation, both of which have their negatives. Classical hand analysis methods such as the work-energy method overestimate the stress for a weight dropped onto the tip of a cantilevered beam. The goal of this project was to formulate analytical equations that were straightforward and easy to implement that would more accurately predict the dynamic stress in this scenario. Using the equations derived from the work-energy method, a modification factor was sought that would allow for a more useful answer.

The approach was to collect experimental data from a weight being dropped onto a cantilevered beam. Different geometries were used as were multiple drop heights. This data was then used to formulate a relationship between drop height and stress. These new equations were then used to modify the original impact equations.

The new equations successfully accounted for the experimental data and are believed to be useful for design purposes. However, the equations were not general and seemed applicable only to the specific setup for which they were formulated.

TABLE OF CONTENTS

LIST OF ILLUSTRATIONS

LIST OF TABLES

LIST OF SYMBOLS

U	Work
F	Force
Δ	Displacement
W	Weight
h	Height
k	Spring Rate
P	Load
L	Length
A	Area
E	Modulus of Elasticity
I	Area Moment of Inertia
σ	Stress
M	Moment

CHAPTER 1

INTRODUCTION

1.1 Introduction

During the design and analysis phase of most projects, many tools may be utilized to determine whether or not structural requirements such as strength and weight are met. These tools might include classical hand analysis, finite element analysis, and testing. When considering cost and time to implement, classical hand analysis should be a first course of action. Finite element software can be very expensive and may be only as good as the engineer sitting at the computer. Testing requires building prototypes and fixtures as well as creating test plans.

It is therefore imperative that engineers are knowledgeable of classical analysis techniques for stress calculations. These have the benefit of being fairly quick and easy to implement. They also give high levels of confidence, providing the structure is not too complicated or there are not too many assumptions regarding loads, constraints, etc. These easy to implement techniques come from knowledge of statics and mechanics of materials.

One area that is not covered under this paradigm is that of dynamic loading. Dynamic analysis is often required for design purposes. Components may be moving and may have dynamic impact with each other. Static components may be subject to abuse loads that are dynamic in nature. It is essential that adequate classical analysis tools are available to ensure the design is effective, functional, and not weight or cost prohibitive. This is especially true in the aerospace industry where weight is a major concern.

There are a few classical methods that can be used for dynamic stress problems. One of these is the impulse-momentum method. This method has the disadvantage of having to know the time of impact, which can only be found experimentally. It also has the disadvantage

of having to know the rebound velocity of the moving bodies which can also only be found experimentally. There are too many factors that have to be known a posteriori for this to be a viable method for classical analysis, especially during the design phase of a project.

Another classical method is the work-energy method. This method utilizes the work done by forces and the conservation of energy to find dynamic forces and displacements which can then be used to find dynamic stress. This will be shown in detail in Chapter 2. It is this method that is the focus of this paper.

1.2 Problem Statement

The purpose of this project is to show that the work-energy method impact equations are too conservative for design purposes in the case of a transverse impact on the tip of a cantilever beam. Empirical tests will be run and the actual stress will be found, which will allow a modification of the impact equations so they can be used for design purposes. Different beam thicknesses will be tested to examine the universality of the results.

The deficiency in the work-energy impact equations was found from a real world problem. It was the analysis of a mount on the exterior of a helicopter. The mount was made from 7050-T7451 aluminum and weighed approximately 10 pounds. It was an “A” frame shape with two extended lugs that were 0.5 inches thick for attachment to the aircraft as shown in Figures 1.1 and 1.2.

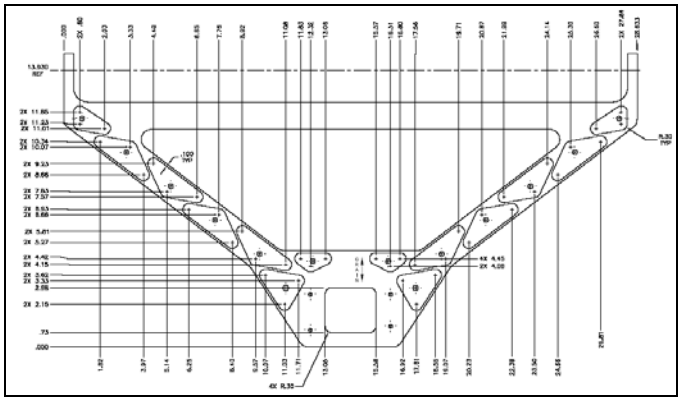

Figure 1.1 The "A" frame component.

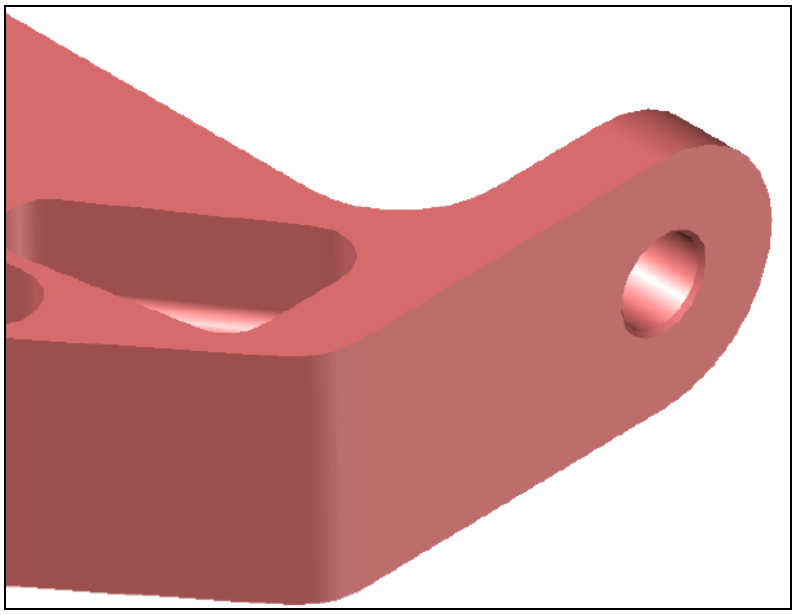

Figure 1.2 One of the extended lugs that attach to the aircraft.

The lugs had to be able to withstand an abuse load if the component was dropped in transit to and from the aircraft. If the lugs suffered permanent deformation, the component would not fit into corresponding brackets and would not be able to mount to the aircraft. It was assumed that the component would be dropped from waist height, so a requirement for the transit drop capability was established as 36 inches.

The lugs were analyzed using classical hand analysis utilizing the aforementioned work-energy impact equations which will be detailed in Chapter 2. The methodology is to find a static stress and displacement from a static load being applied. An impact factor, which is a function of drop height, is then found which is subsequently multiplied by the static stress to find the dynamic stress. The method is rather straightforward and easy to apply if the problem is slightly simplified. In this case, the problem was simplified to that of a fixed cantilever beam with the dimensions of the extended lug having 10 pounds dropped onto it. The stress from this methodology is conservative, but it was assumed that the answer would be reasonable enough for design purposes. It was found that the methodology yielded a stress that was extremely

high and was of no use in the design. An adequate theoretical solution could not be found in a timely manner; however, the requirement was eventually dropped.

This did bring up the issue of the need for a simple methodology to analyze impact problems of this nature. Most stress analysis equations in industry use are straightforward, algebraic, and fairly easy to implement. It is desirable that an impact equation that yields reasonable results would fit these criteria. The goal of this project is to modify the impact equations using empirical data to make the results given more reasonable for design purposes.

1.3 Literature Survey

A review of published literature shows there is activity regarding transverse impact on beams; however, specifically addressing the impact factors of the work-energy method is quite limited.

Usuki and Maki [1] formulated an equation of motion using higher order beam theory. This method examined the effects of nonlinear components of axial-warping which are not addressed in conventional approaches. Although the transverse impact is directly relevant, the formulation used is mathematically demanding and does meet the above mentioned criteria.

Chen, Zheng, Xue, Tang, and Wang [2] analyzed an unrestrained Timoshenko beam that undergoes transverse impact. They found the dynamic responses of the beam are composed of rigid and elastic responses. The elastic responses found are very similar to the dynamic responses of a simply supported beam. The momentum transfer was also investigated. It was found that the momentum of the rigid response equaled the moving rigid body momentum before impact.

Szuladzinski [3] investigated the inelastic range of the beam material under a distributed pulse load. Four support conditions were considered looked at including the clamped-free, or cantilevered beam. It was found that the material model used had a large influence on the numerical results. The accuracy of the calculations was improved by a transition to a different material model which improved the energy balance. The investigation

presented in this thesis deals with the elastic range only, as that is one of the assumptions made for the present work-energy method presented in Chapter 2.

Wang, So, and Chan [4] considered the dynamic normal and shear stresses in a beam in which contributions are made from standing waves. According to the authors, "...the study of dynamic stresses in a beam is scarce." They investigated two time durations for the impulse loadings. The results showed that certain wave components are responsible for certain crack growth modes. They also found a difference in wave contribution based on impulse duration. The boundary conditions were also found to affect the contributions of the wave components to the dynamic stress.

The most relevant research was performed by Suzuki [5]. The dynamic load factors of cantilevered beams were investigated. A theoretical approach was empirically tested. The theoretical derivation was not given so it is unknown what method was used. For the testing, the weight was not dropped from a height, but applied as if static and released abruptly. It was found that the solid viscosity and frequency of the member have an important effect on the dynamic stress. The results showed that as the frequency of the beam was increased, the dynamic load factor decreased. The results were limited in scope as the effect of drop height was not investigated.

CHAPTER 2

THEORETICAL ANALYSIS

2.1 Impact Equations

When one object strikes another, impact occurs. This means that large forces are developed that last for only a short period of time. The basic approach to analyzing these forces and subsequent stresses that they induce is done with a work-energy method. Conservation of energy is assumed during the impact, which means there is no energy loss. The derivation in this section is from [6].

To develop this methodology, the work of a force must be found. A force does work when it experiences a displacement *dx* in the same direction the force is acting. The work performed is defined as the scalar

$$U_e = \int_0^x F dx \tag{1}$$

An axial force is applied to the end of a bar, shown in Figure 2.1, and the work done will be calculated.

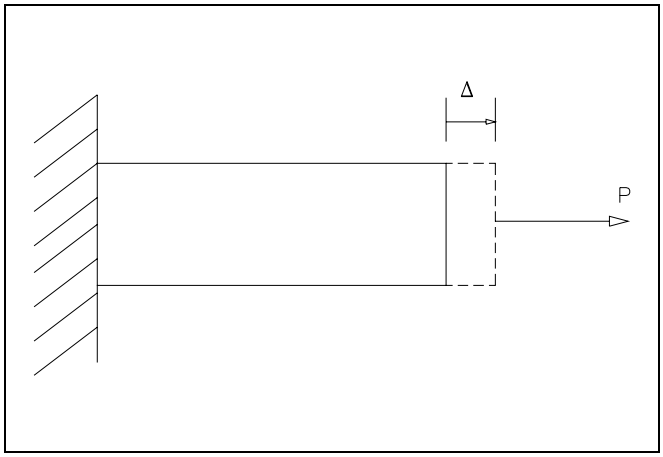

Figure 2.1 The load *P* causes the displacement Δ.

As the force is gradually increased from zero to a final value of *P*, the end of the bar is displaced by the distance Δ. The material will be assumed to behave in a linear-elastic manner. As such, the force is directly proportional to the displacement

$$F = \left(\frac{P}{\Delta}\right)x \tag{2}$$

Substituting equation (1) into equation (2) yields

$$U_e = \int_0^{\Delta}\left(\frac{P}{\Delta}\right)x\,dx \tag{3}$$

The work performed by the force on the bar is

$$U_e = \frac{1}{2}P\Delta \tag{4}$$

To continue the development, the conservation of energy will be added. A block will be dropped on a spring as shown in Figure 2.2.

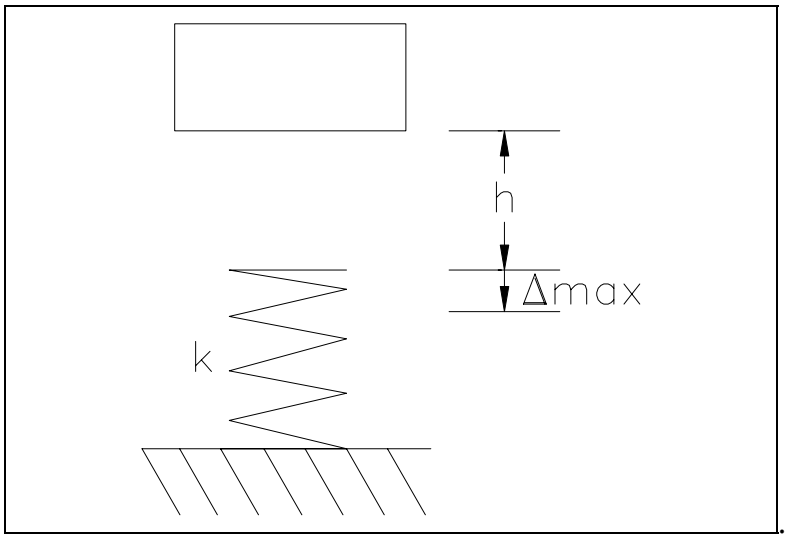

Figure 2.2 The block drops onto the spring from height *h*.

The block falls from an initial position *h* and impacts the spring. During the impact the spring is compressed a distance Δ_{max} before coming to rest. The two assumptions that are made are that the spring is massless and responds elastically. Thus, the conservation of energy requires that the energy of the falling block is turned into strain energy in the spring. This means that the work done by gravity on the falling block is equal to the work required to displace the spring by an amount Δ_{max}. The work done by gravity on the falling block is the weight of the block times the distance it falls, $W(h + \Delta_{max})$. The spring equation relates force to displacement through the relation

$$F = k\Delta_{\max} \tag{5}$$

Now the conservation of energy is applied along with equations (4) and (5)

$$U_e = U_i \tag{6}$$

$$W\left(h + \Delta_{\max}\right) = \frac{1}{2}\left(k\Delta_{\max}\right)\Delta_{\max} \tag{7}$$

$$W\left(h + \Delta_{\max}\right) = \frac{1}{2}k\Delta_{\max}^2 \tag{8}$$

$$\Delta_{\max}^2 - \frac{2W}{k}\Delta_{\max} - \frac{2Wh}{k} = 0 \tag{9}$$

This quadratic equation is then solved for Δ_{max}. The maximum root being

$$\Delta_{\max} = \frac{W}{k} + \sqrt{\left(\frac{W}{k}\right)^2 + 2\left(\frac{W}{k}\right)h} \tag{10}$$

From equation (5), if the weight is applied statically to the spring

$$\Delta_{st} = \frac{W}{k} \tag{11}$$

Incorporating equation (11) into equation (10) yields

$$\Delta_{\max} = \Delta_{st} + \sqrt{\Delta_{st}^2 + 2\Delta_{st}h} \tag{12}$$

Simplifying,

$$\Delta_{\max} = \Delta_{st}\left[1+\sqrt{1+2\left(\frac{h}{\Delta_{st}}\right)}\right] \tag{13}$$

After Δ_{max} is found from equation (13), the maximum force can be found from equation (5).

There are several assumptions that must be made in order to apply this method to a deformable body subjected to impact. It must be assumed that the moving body is rigid like the block in the above model. Also, the stationary body is assumed to be deformable like the spring and behaves in a linear-elastic manner. During the collision, it is assumed that no energy is lost due to sound, heat, or plastic deformations. Lastly, it is assumed that the bodies remain in contact when the collision occurs until the elastic body reaches its maximum deflection. These assumptions will result in a conservative estimate of the deflection and stress experienced by the elastic body.

Problems of this nature can be solved by a more direct approach than solving for work and energy. The elastic body can be modeled as an equivalent spring. Taking the above example and assuming the spring is a column with displacement of

$$\Delta = \frac{PL}{AE} \tag{14}$$

and therefore has a spring stiffness of

$$k = \frac{AE}{L} \tag{15}$$

A spring having the stiffness given in equation (15) would be displaced by the same amount from the force *P*, specifically

$$\Delta = \frac{P}{k} \tag{16}$$

Pertinent to the current discussion, the spring can also be a cantilevered beam subject to a transverse load at the tip resulting in a tip deflection of

$$\Delta = \frac{-PL^3}{3EI} \tag{17}$$

and therefore has a spring stiffness of

$$k = \frac{3EI}{L^3} \tag{18}$$

However, it is unnecessary to find the equivalent spring stiffness to apply equation (13). All that is required to find the dynamic displacement, Δ_{max}, is to find the static displacement, Δ_{st}, due to the weight, W, of the object resting on the elastic member. After finding Δ_{max}, the dynamic force is found from

$$P_{\max} = k\Delta_{\max} \tag{19}$$

P_{max} is to be considered an equivalent static load which will lead to the maximum stress in the member. The ratio of this equivalent static load, P_{max}, to the weight of the rigid body, W, is the impact factor, n, and is expressed as

$$n = 1 + \sqrt{1 + 2\left(\frac{h}{\Delta_{st}}\right)} \tag{20}$$

The impact factor, n, allows a statically applied load to be treated as a dynamic load by magnifying the static load. To calculate the dynamic impact deflection, the static deflection is simply multiplied by the impact factor, n.

$$\Delta_{\max} = n\Delta_{st} \tag{21}$$

To calculate the dynamic impact stress, the static stress is multiplied by the impact factor, n.

$$\sigma_{\max} = n\sigma_{st} \tag{22}$$

2.2 Sample Problem

This sample problem will illustrate how the equations are used. This problem is taken directly from the initial helicopter mount problem and is the basic setup for the experimental analysis.

Consider a cantilevered 2024-T3 aluminum beam 2 inches long by 1.75 inches wide and 0.5 inches thick. The modulus of elasticity is 9.9E6 psi, the yield strength is 42 ksi, and the ultimate strength is 64 ksi. A 10 lb weight dropped from a height of 10 inches onto the tip of the beam.

The first step is to find the static displacement using the standard beam deflection equation.

$$\Delta_{st} = \frac{-PL^3}{3EI} \tag{23}$$

$$\Delta_{st} = \frac{-10*2^3}{3*9.9E6*0.01823}$$

Δ_{st} = -0.000148 in (The absolute value of the deflection will be used.)

The static stress is now calculated.

The flexure formula will be used to find the stress at the attachment point of the beam.

$$\sigma_{st} = \frac{Mc}{I} \tag{24}$$

$$\sigma_{st} = \frac{10*2*0.25}{0.01823}$$

σ_{st} = 274.3 psi

The impact factor, *n*, will now be calculated and then multiplied with both the static deflection and static stress to get the impact deflection and stress. Using equation (20)

$$n = 1 + \sqrt{1 + 2*\left(\frac{h}{\Delta_{st}}\right)}$$

$$n = 1 + \sqrt{1 + 2 * \left(\frac{10}{0.000148} \right)}$$

n = 368

The impact deflection and stress are then found.

$$\Delta_{\max} = n\Delta_{st}$$

$$\Delta_{\max} = 368 * 0.000148$$

$$\Delta_{\max} = 0.054 \text{ in}$$

$$\sigma_{\max} = n\sigma_{st}$$

$$\sigma_{\max} = 368 * 274.3$$

$$\sigma_{\max} = 100.9 \text{ ksi}$$

The bending modulus of yield is calculated as follows using the Cozzone simplified procedure from [7].

$$F_b = \frac{M_b c}{I}$$

$$F_b = f_m + f_o(k - 1) \quad (25)$$

k = 1.5 for rectangular cross sections [Figure C3.7, reference 7]

f_m = 42 ksi

f_o = 20 ksi [Figure C3.13, reference 7]

$$F_b = 42 + 20 * (1.5 - 1)$$

F_b = 52 ksi

The ultimate bending modulus of rupture is calculated as follows also using the Cozzone simplified procedure.

$$F_b = \frac{M_b c}{I}$$

$$F_b = f_m + f_o(k-1)$$

k = 1.5 for rectangular cross sections [Figure C3.7, reference 7]

f_m = 64 ksi

f_o = 52 ksi [Figure C3.13, reference 7]

$$F_b = 64 + 52 * (1.5 - 1)$$

F_b = 90 ksi

The calculated stress is 10 ksi greater than the ultimate bending modulus of rupture. Taken at face value, this is predicting a catastrophic failure from a 10 inch drop. This is obviously not what actually happens.

There is an adjustment factor from [8] to account for energy losses during the impact. This approach uses conservation of momentum and is expressed in the following equation.

$$K = \frac{1 + \frac{33M_1}{140M}}{\left(1 + \frac{3M_1}{8M}\right)^2} \tag{26}$$

Where M_1 is the mass of the cantilever beam and M is the mass of the moving body that strikes the beam. This gives a K value of .99 which is then multiplied with h in equation (20). This in turn gives an impact factor of 367, which is less than a 1% difference from the previous value of n.

2.3 Theoretical Results

The above equations and methodology were applied to various drop heights on a similar beam from the sample problem. The material is the same as that used for the experimental tests. Three beam thicknesses were analyzed. The results are shown in Figures 2.3 through 2.5. As can be seen, the stresses are quite high.

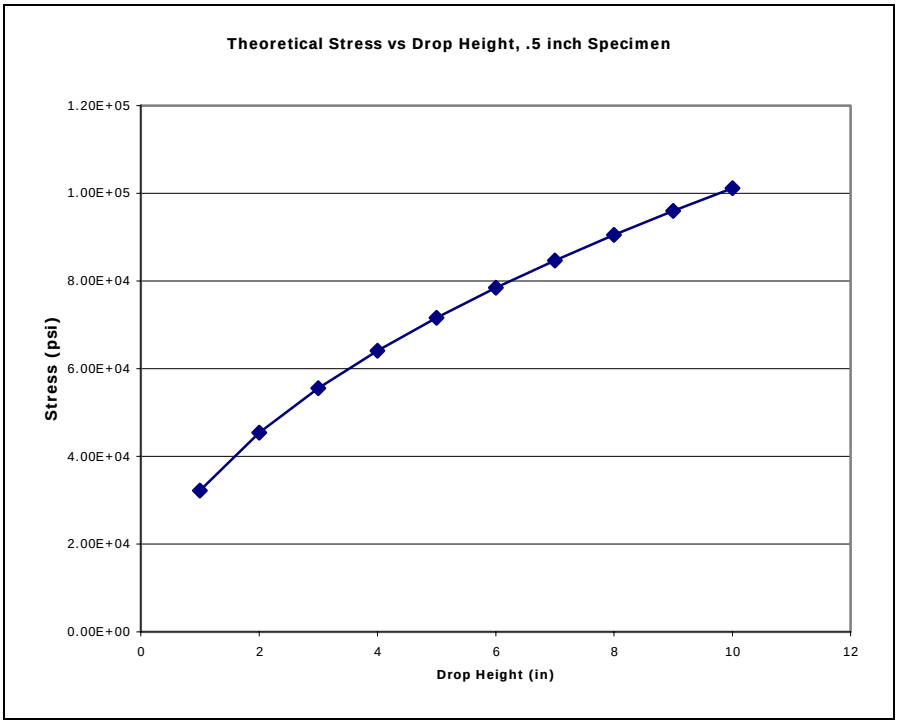

Figure 2.3 Stress as a function of drop height for the .50 inch specimen.

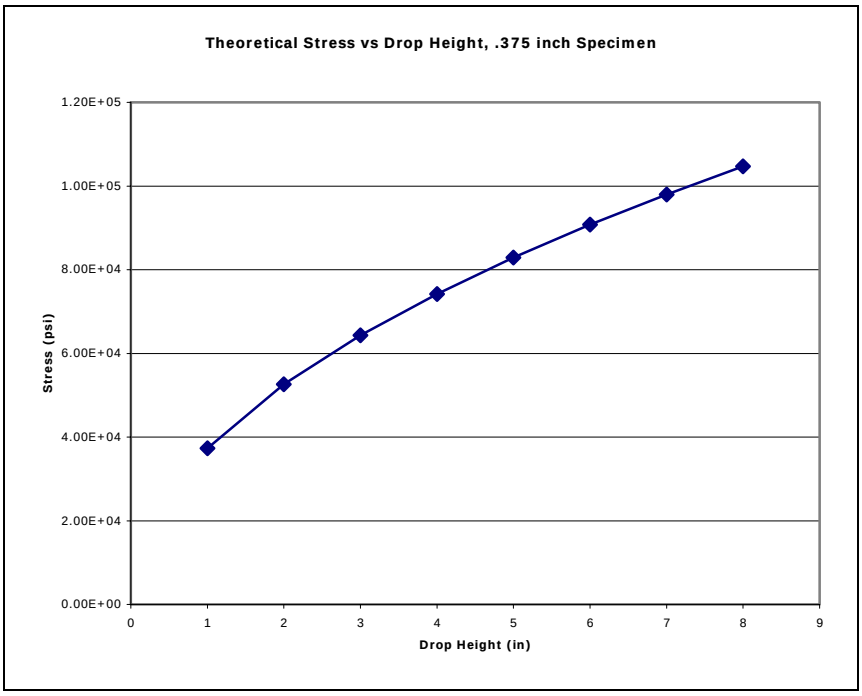

Figure 2.4 Stress as a function of drop height for the .375 inch specimen.

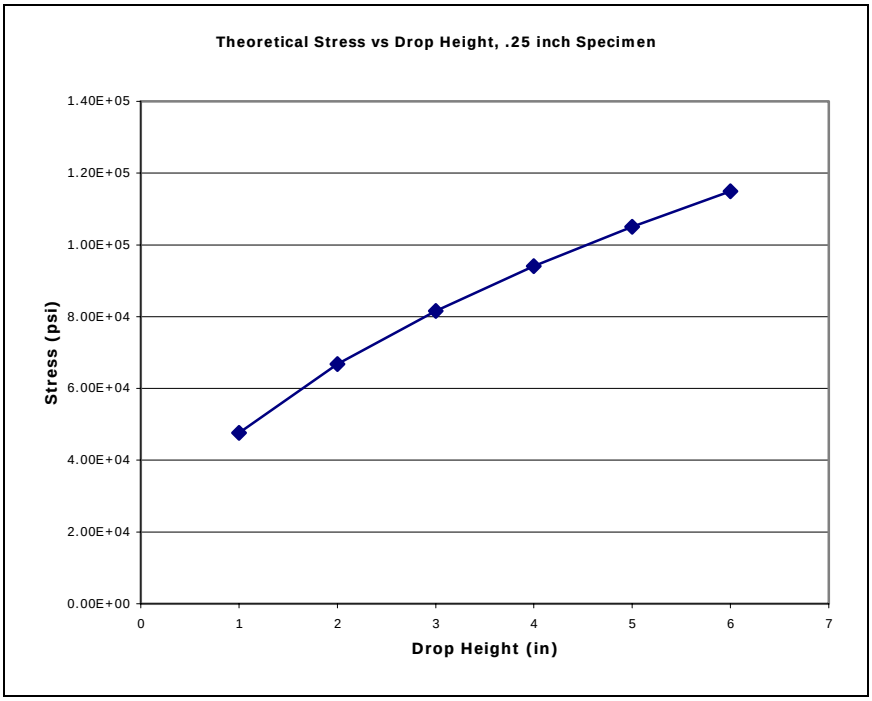

Figure 2.5 Stress as a function of drop height for the .25 inch specimen.

CHAPTER 3

EXPERIMENTAL ANALYSIS

3.1 Test Setup

A test setup was created to mimic the example problem in Chapter 2 and to give insight into the initial problem presented in Chapter 1. A test fixture was created that allowed for the controlled free fall of a 10 pound weight from various heights. A second fixture was created to hold a test specimen in a cantilevered position and made to interface with the first fixture. The two fixtures together would allow for a replication of the example problem, specifically, a falling mass impacting the tip of a cantilever beam. The fixtures are shown in Figures 3.1 through 3.3.

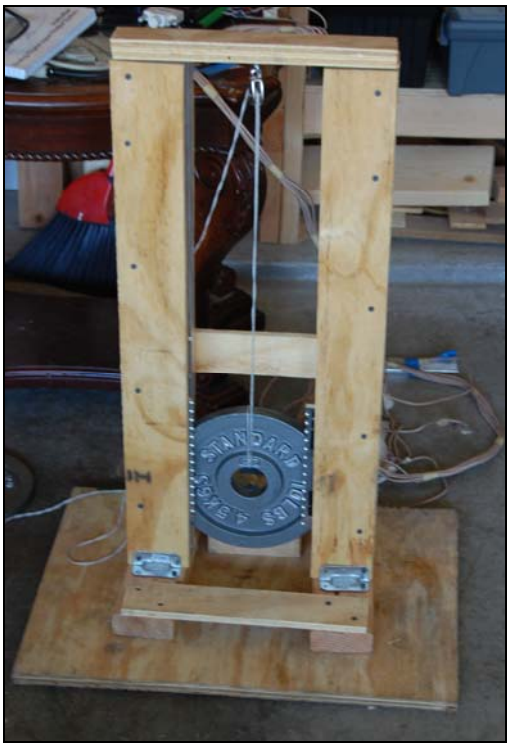

Figure 3.1 The test fixtures holding the dropped weight.

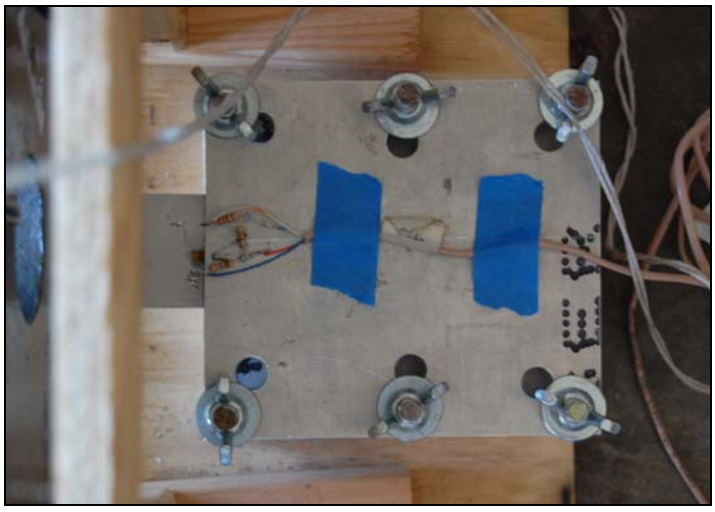

Figure 3.2 The test fixture holding the test specimen.

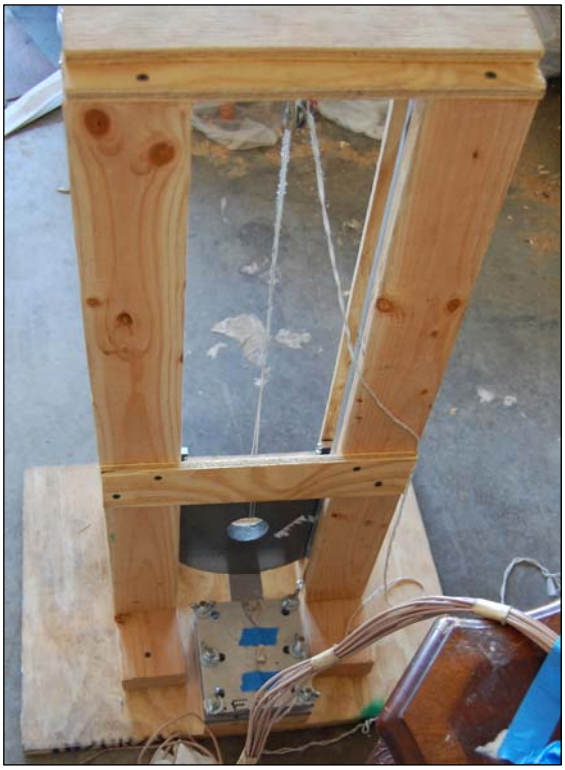

Figure 3.3 Both fixtures together with a test specimen.

The test specimens consisted of three different geometries and two types of aluminum. The different specimens were used to gather more data and attempt to gain more insight into

the problem. The only difference in geometry was the specimen thickness. This was to keep the number of variables low. Also only 2 different materials were used for the same reason. The specimen geometry and material is shown in Table 3.1.

Table 3.1 Test Specimen geometry and material properties.

Test Specimen	Height (in)	Width (in)	Material	Yield Strength (ksi)	Ultimate Strenght (ksi)	Modulus of Elasticity (psi)
1	0.5	1.75	6061-T651 alum	35	42	9.90E+06
2	0.375	1.75	6061-T651 alum	35	42	9.90E+06
3	0.25	1.75	2024-T351 alum	42	64	1.07E+07

The test specimens were affixed with strain gages on the upper surface near the root end. The strain gages were monitored with data acquisition hardware and software. The equipment list is shown in Table 3.2.

Table 3.2 The software and hardware equipment list.

Software	Instrunet Version 3.0.0.12
Hardware	PCI Controller i200, S/N 54138, calibrated 12/06/07
	device #i100, S/N 50011, calibrated 12/12/07
	inet #330 electrical isolator
	Omega strain gages, 350 ohm, P/N SGD-2/350-LY13

The test specimens were inserted into the fixture as to be cantilevered 2 inches. The weight was then dropped onto the tip end of the specimen from 1 to 10 inches at intervals of 1 inch. The data was recorded with a sampling rate of 10,000 samples per second.

There was an initial calibration of one of the gages. A known and increasing load was applied to the test specimen. The applied load and corresponding measured stress are shown in Figure 3.4.

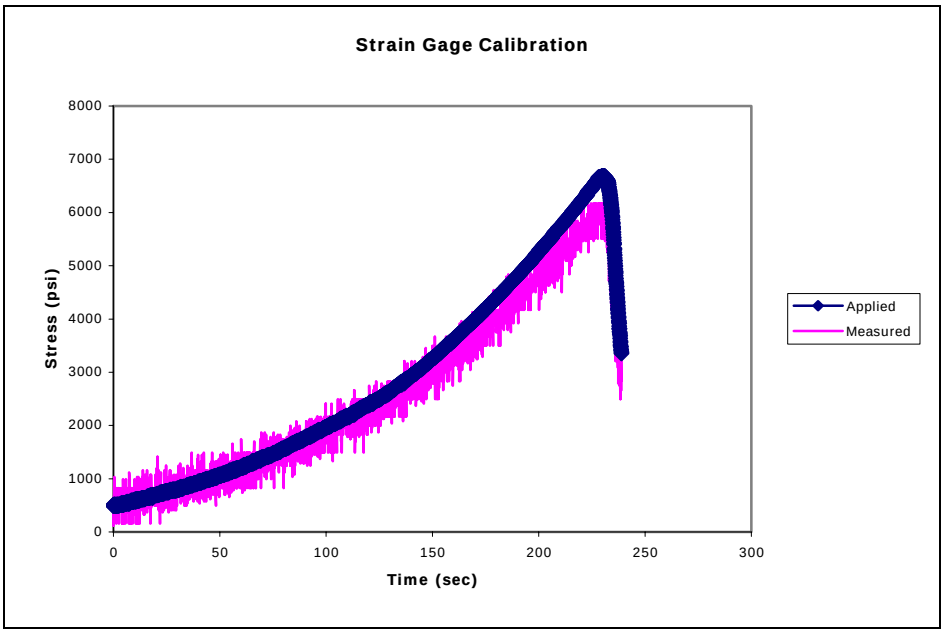

Figure 3.4 The applied load and measured stress for the strain gage calibration.

The Measured strain followed the applied load very well and the peak value measured was only 8% under the applied load. This was deemed acceptable and that the strain gage placement and application would yield adequate results.

3.2 Test Results

The results were collected for multiple specimens using multiple strain gages. The results from a typical drop on a .500 inch specimen are shown in Figure 3.5.

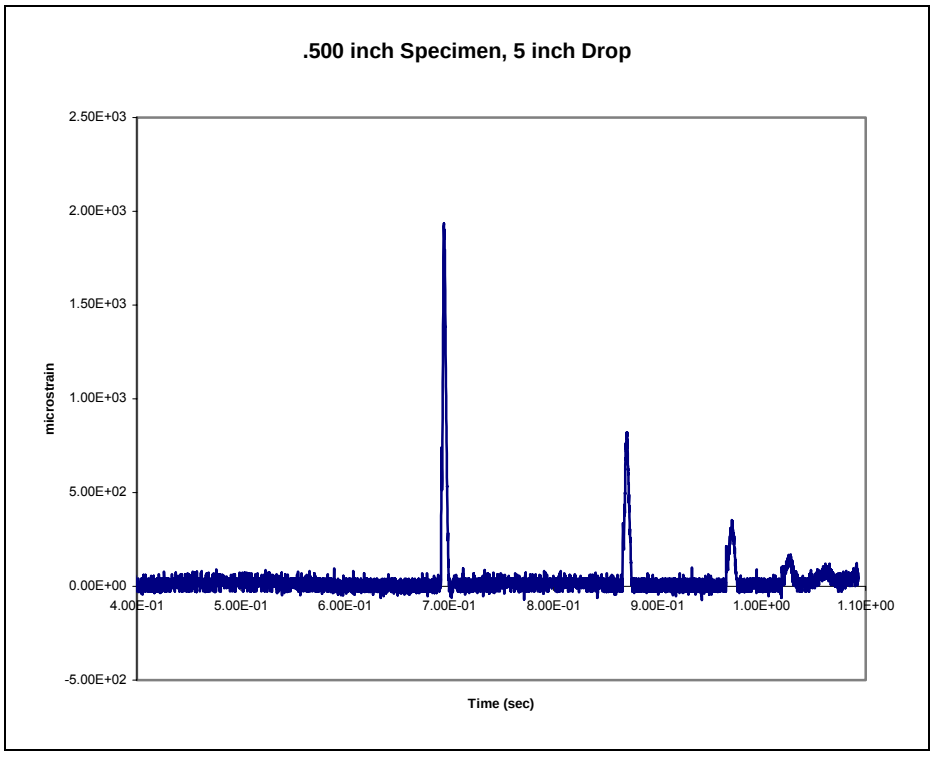

Figure 3.5 A typical result of the impact of a 5 inch drop onto a half inch specimen.

As can be seen from the figure, there is an initial spike in strain and then subsequent spikes later in time. This corresponds to the initial impact and the weight bouncing on the beam. Only the stress from the first spike, or initial impact, was used in subsequent calculations. A close-up of the first spike reveals its time duration and the waveform of the strain as shown in Figure 3.6.

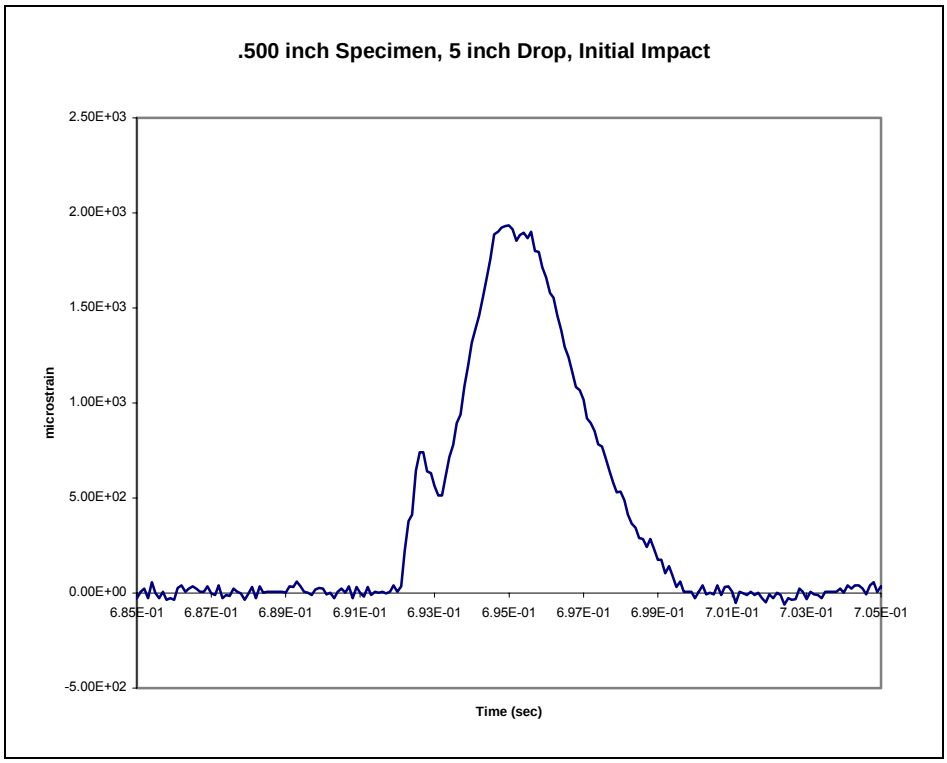

Figure 3.6 A close-up view of the initial impact from Figure 3.2.1.

The figure shows that the impact strain lasted approximately 0.008 seconds and peaked at approximately 2,000 μstrain. From this data, the sampling rate was determined to be adequate and there would not be any large spikes being missed by undersampling. The waveform shows an initial peak before the main peak values. This was assumed to be a dynamic effect from the particular geometry of the beam itself. This was confirmed by comparing to waveforms from the other specimens. They are shown fin Figures 3.7 and 3.8.

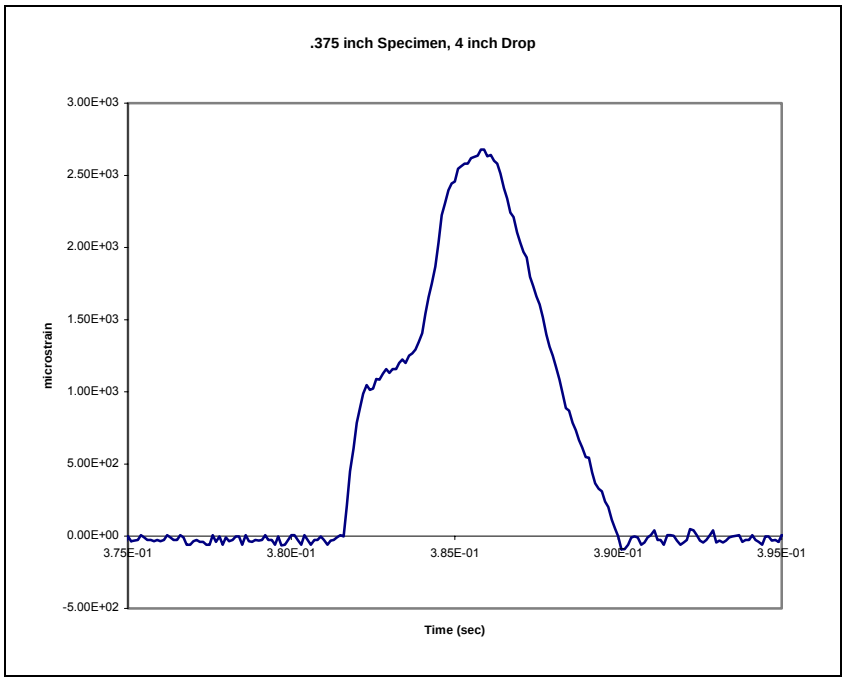

Figure 3.7 The typical waveform of the .375 inch specimen impact.

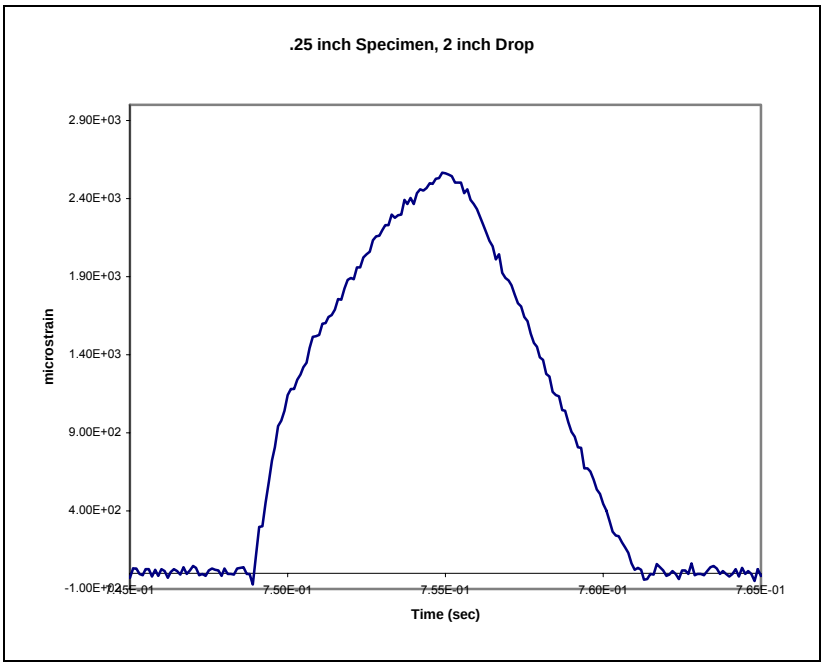

Figure 3.8 The typical waveform of the .250 inch specimen impact.

Figure 3.6 shows the prominent peak before the maximum values for the .500 inch specimen. The .375 inch specimen shows the peak flattening in Figure 3.7. The .250 inch specimen has no peak at all before the maximum values as shown in Figure 3.8. This shows that the peak is dependent on specimen geometry. Only the maximum values recorded were analyzed, so no further analysis of the waveform was deemed necessary.

The .500 inch specimen had drop heights from 1 to 10 inches with intervals of 1 inch. The recorded strain was multiplied by the modulus of elasticity to get stress. The drop test was run for 11 trials. Two different specimens and 4 different strain gages were used. The results were very consistent between specimens and gages. The results for a typical test are shown in Figure 3.9. A compilation of the results is shown in Figure 3.10.

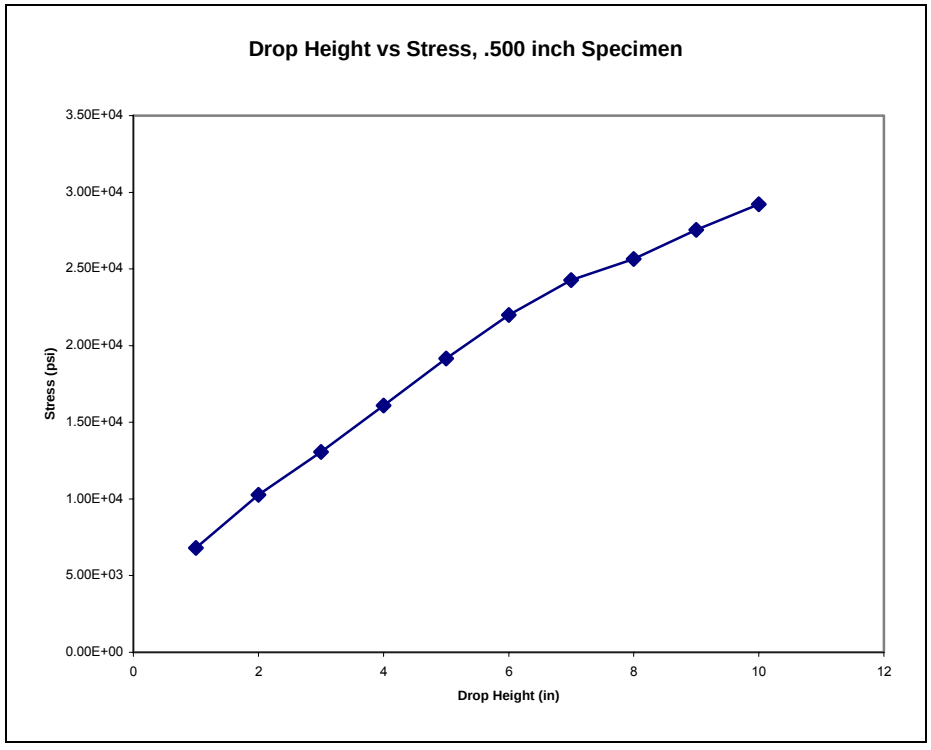

Figure 3.9 The relationship between drop height and stress for the .500 inch specimen.

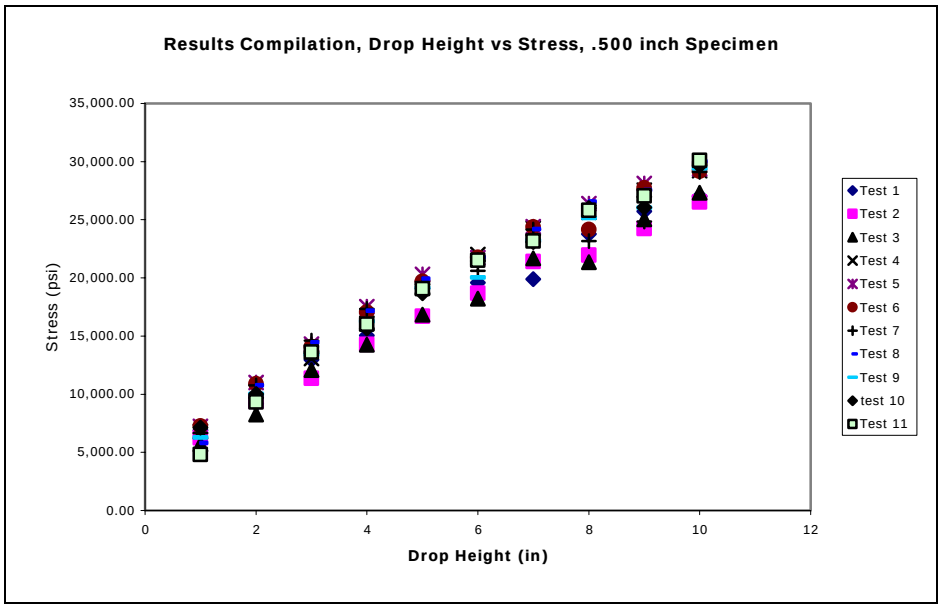

Figure 3.10 The total results for the .500 inch specimen.

The results are fairly consistent from one trial to the next. There are a few outlying data points. The overall relationship is consistent as are the peak values. There is approximately a 12% difference between the highest maximum stress and the lowest maximum stress. The same methodology was performed for the .375 inch and .25 inch specimens.

The .375 inch specimen had drop heights from 1 to 8 inches with intervals of 1 inch. The drop test was run for 4 trials. There were 2 different specimens and 2 different strain gages used to collect the data. The results for a typical test are shown in Figure 3.11. A compilation of the results is shown in Figure 3.12.

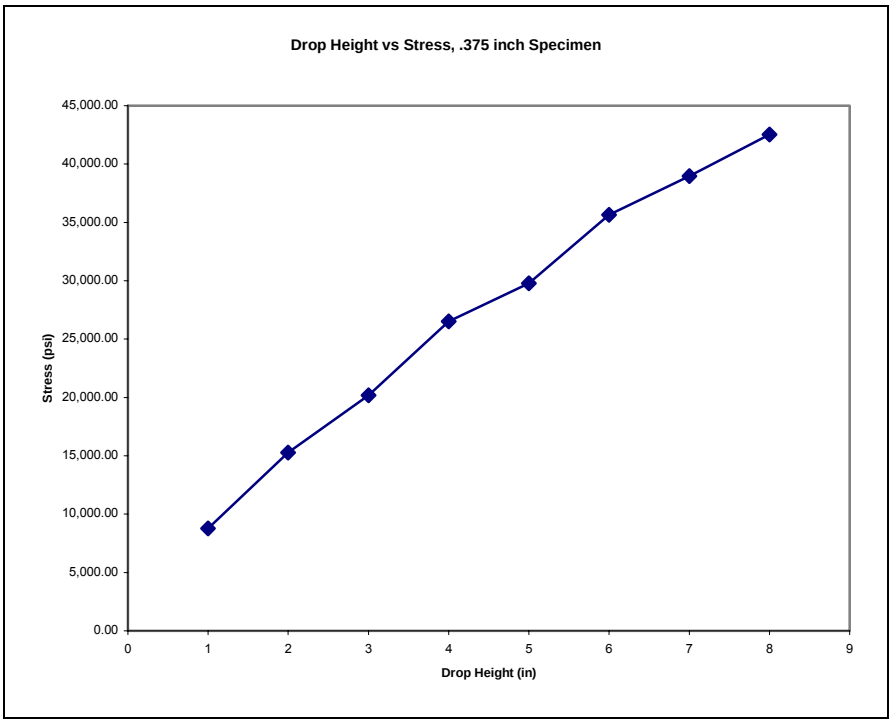

Figure 3.11 The relationship between drop height and stress for the .375 inch specimen.

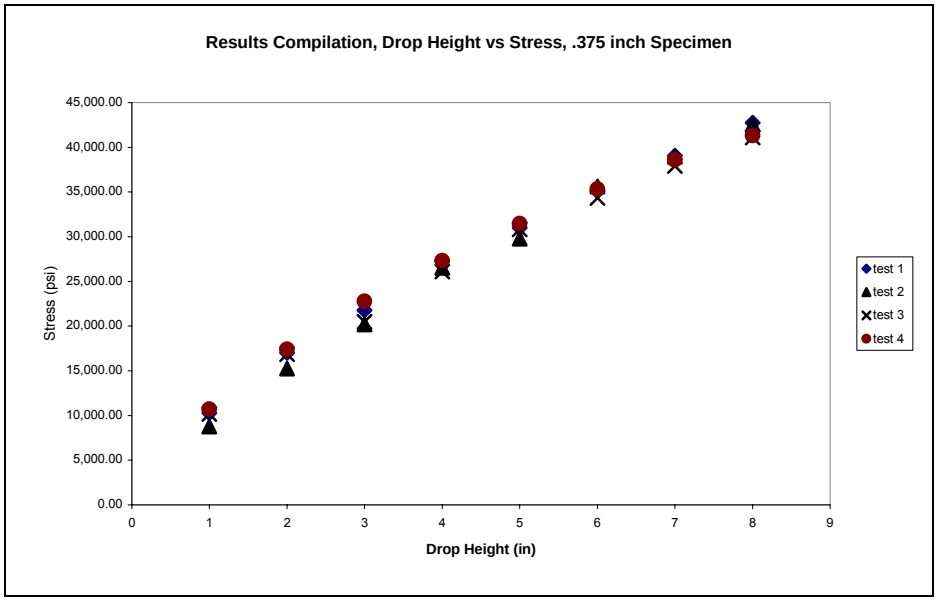

Figure 3.12 The total results for the .375 inch specimen.

The results are consistent from one trial to the next. There is approximately a 4% difference between the highest maximum stress and the lowest maximum stress. The maximum drop height was lowered from 10 inches to 8 inches to avoid yielding the specimen.

The .25 inch specimen had drop heights from 1 to 6 inches with intervals of 1 inch. The drop test was run for 3 trials. There were 2 different specimens and 2 different strain gages used to collect the data. The results for a typical test are shown in Figure 3.13. A compilation of the results is shown in Figure 3.14.

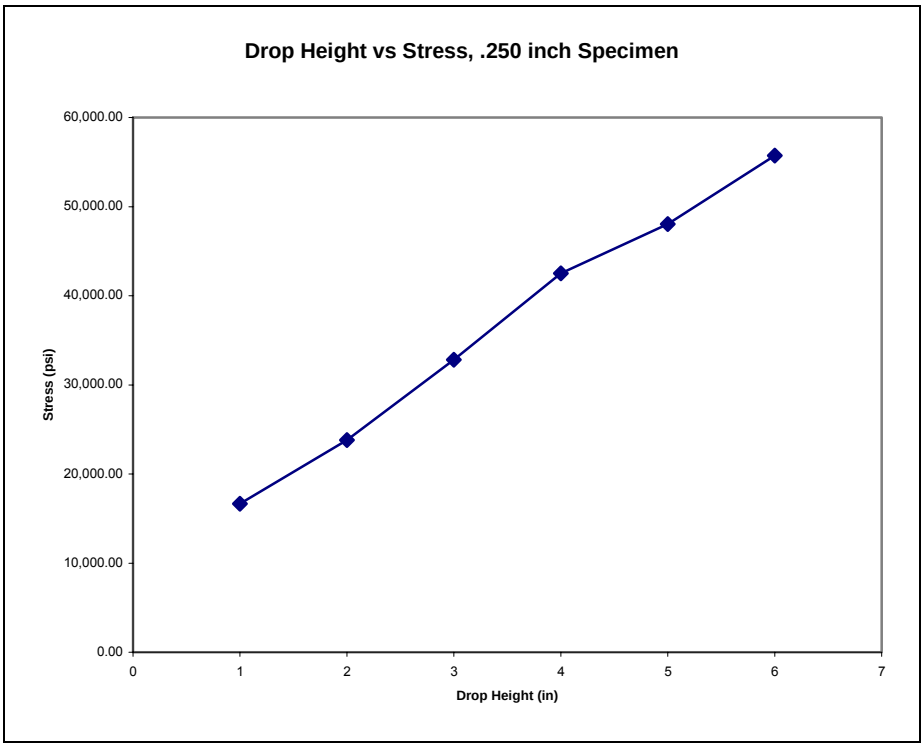

Figure 3.13 The relationship between drop height and stress for the .25 inch specimen.

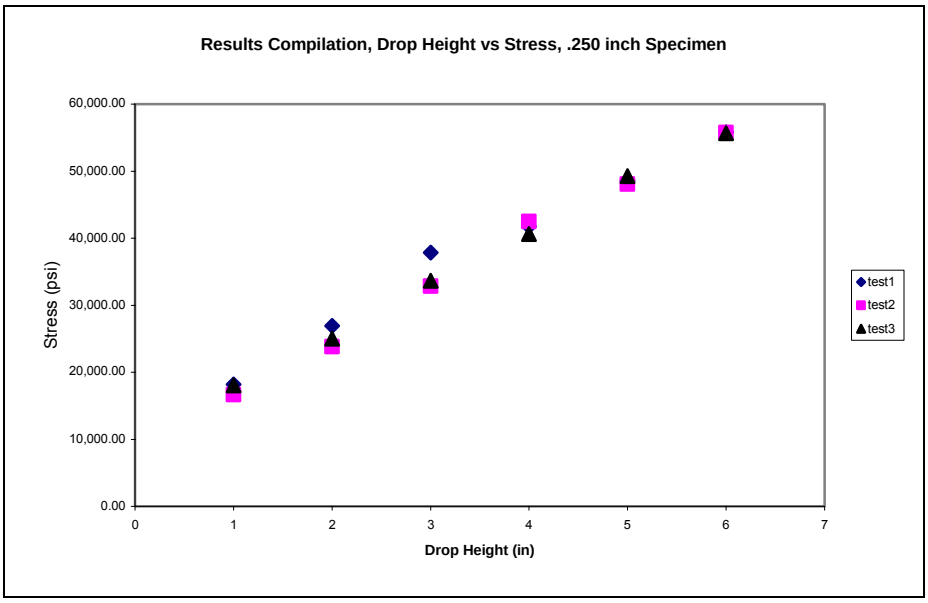

Figure 3.14 The total results for the .25 inch specimen.

3.3 FEM Results

A finite element analysis was performed as independent verification of the empirical results and methodology [9]. The analysis was performed in Ansys-LSDyna and replicated the test setup. A cantilever beam with a .500 inch thickness had a 10 lb weight dropped on the tip from a height of 5 inches. The expected result from the analytical solution is a stress of approximately 70,000 psi. The expected result from the empirical results is approximately 20,000 psi. The setup is shown in Figure 3.15. The stress plot is shown in Figure 3.16.

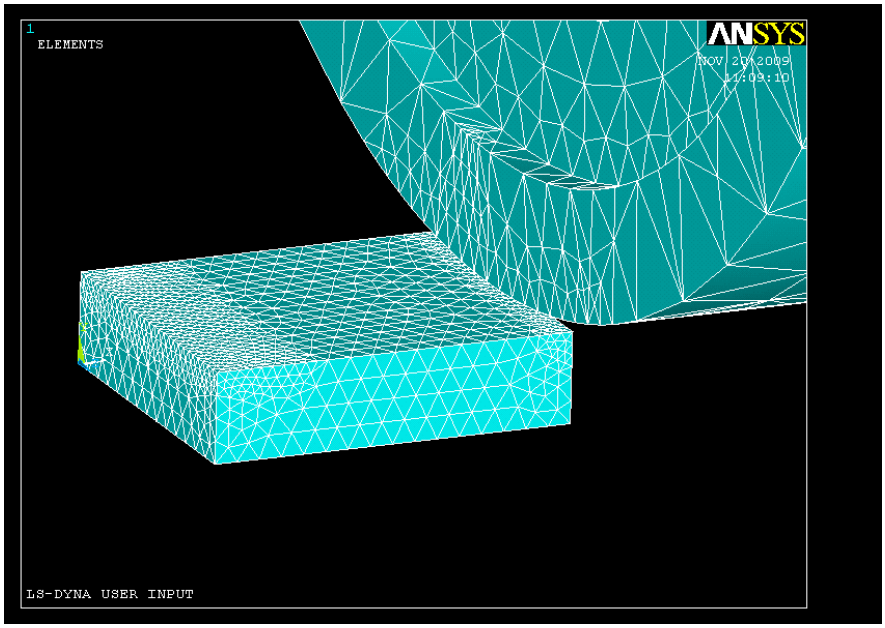

Figure 3.15 The FEM setup.

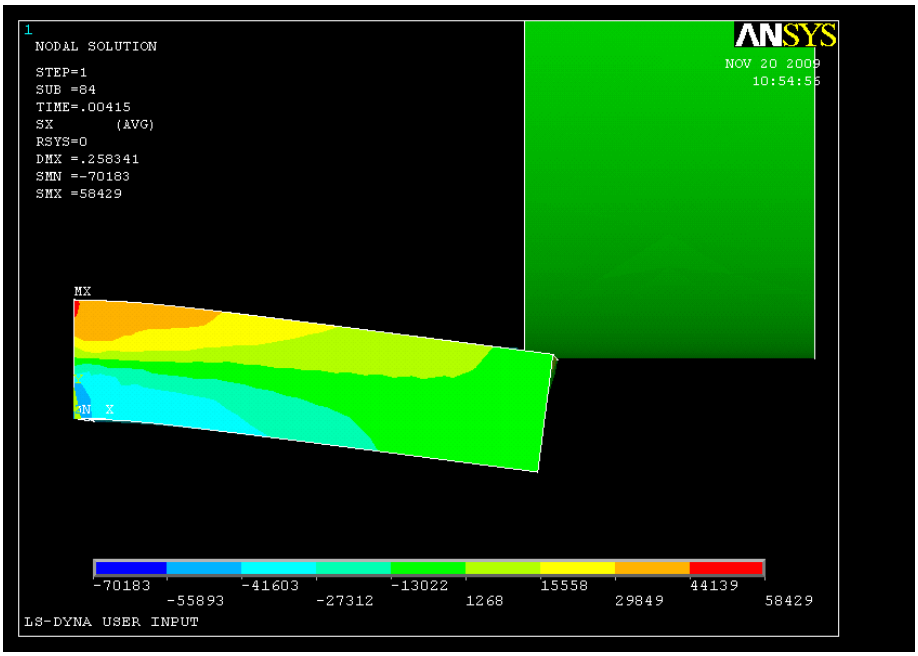

Figure 3.16 The stress distribution results of the FEM.

The area that would contain the strain gage shows a stress of approximately 30,000 psi. This result agrees much more closely with the empirical results than the analytical results. This independent verification gives confidence to the empirical results and methodology.

CHAPTER 4

THEORETICAL AND EXPERIMENTAL COMPARISON

The theoretical approach was used to establish a relationship between drop height and stress. This is compared to single trial experimental results for all 3 specimen geometries as shown in Figures 4.1 through 4.3.

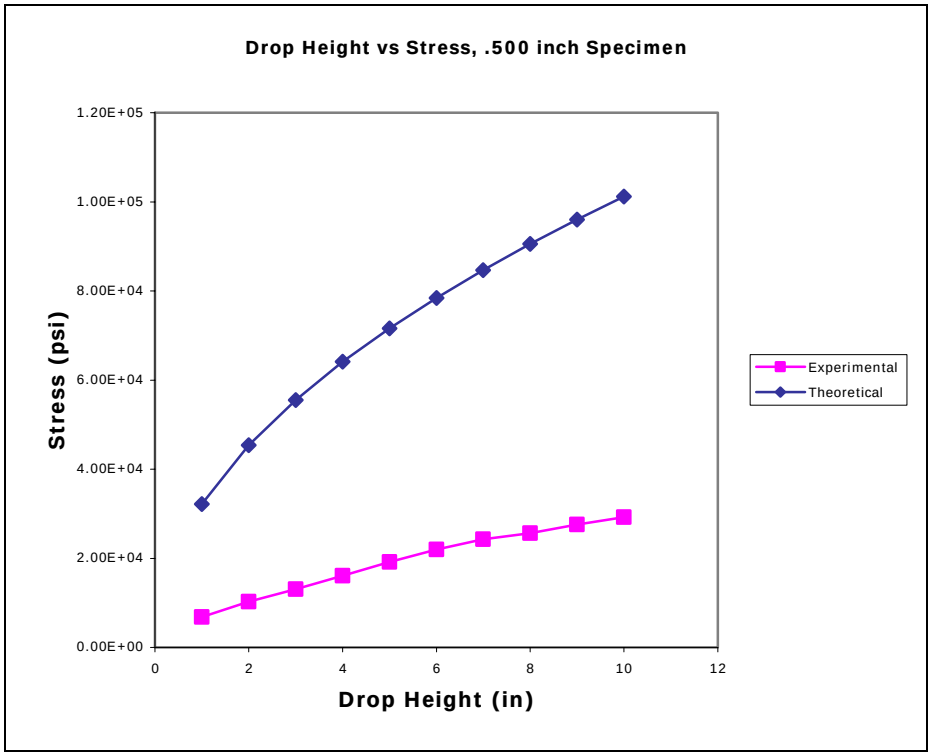

Figure 4.1 The theoretical vs experimental results for the .500 inch specimen.

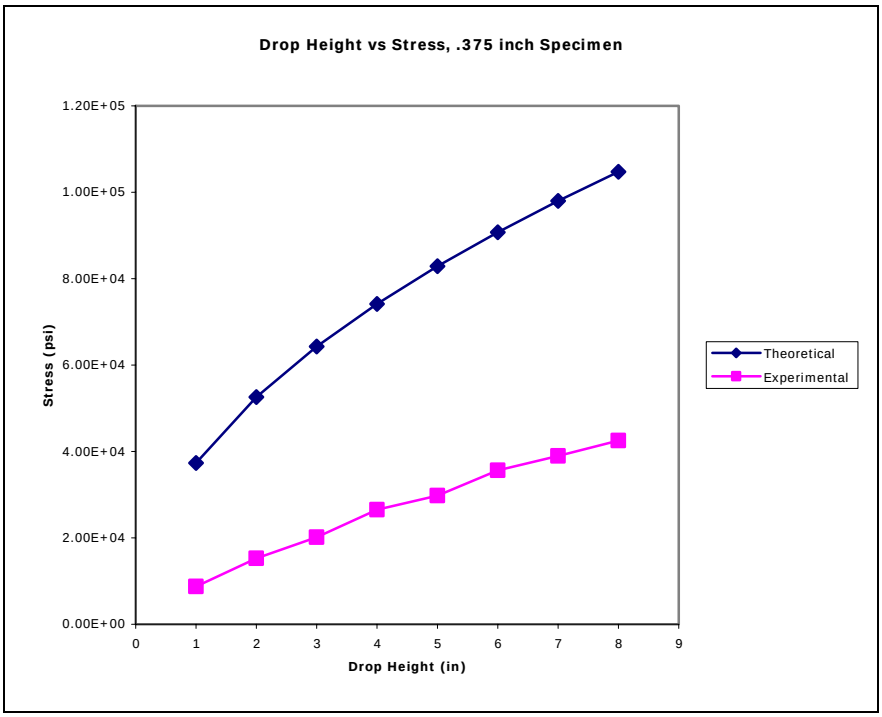

Figure 4.2 The theoretical vs. experimental results for the .375 inch specimen.

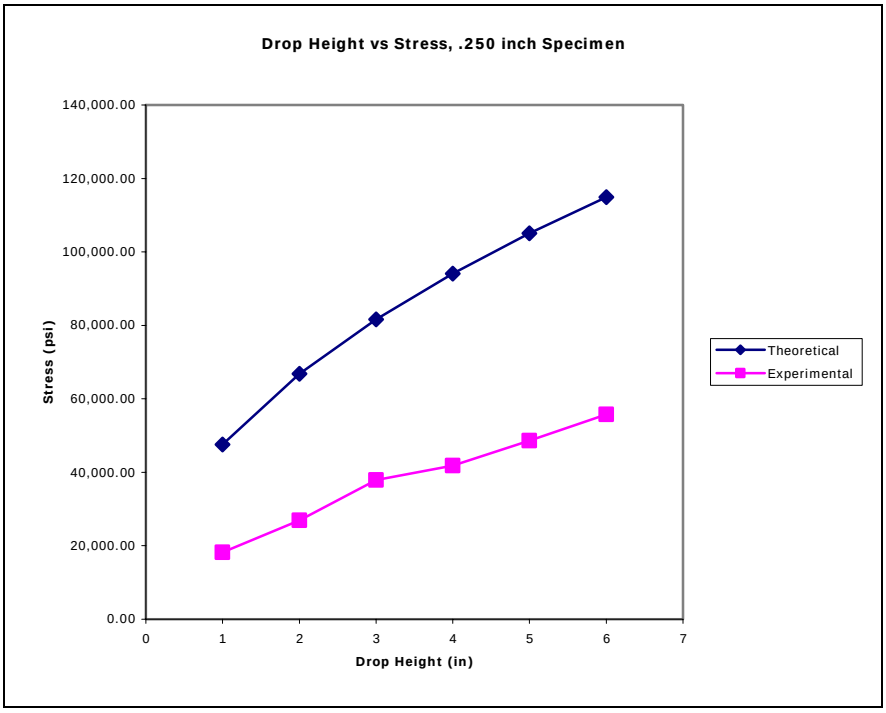

Figure 4.3 The theoretical vs experimental results for the .250 inch specimen.

As can be seen from the figures, the theoretical stress is much higher than the actual stress. This is the discrepancy noted earlier that does not allow the equations from Chapter 2 to be utilized for design purposes. The goal is to modify the equations from Chapter 2 to fit the experimental data. This was achieved by finding the equations that best fit the experimental data and gave useable information. These equations are shown below.

For the .500 inch thick specimen:

$$\sigma = 7{,}276h^{0.6} \tag{27}$$

For the .375 inch thick specimen:

$$\sigma = 11{,}000h^{0.65} \tag{28}$$

For the .250 inch thick specimen:

$$\sigma = 18{,}000h^{0.62} \tag{29}$$

These equations were used to find modification factors to the original impact equations. These modification factors were applied to the static displacement portion of the impact factor. The modified impact factors are shown below.

For the .500 inch thick specimen:

$$n = 1 + \left(1 + 2\left(\frac{h}{57.93\Delta_{st}}\right)\right)^{0.6} \tag{30}$$

For the .375 inch thick specimen:

$$n = 1 + \left(1 + 2\left(\frac{h}{47.16\Delta_{st}}\right)\right)^{0.65} \tag{31}$$

For the .250 inch thick specimen:

$$n = 1 + \left(1 + 2\left(\frac{h}{20.1\Delta_{st}}\right)\right)^{0.62} \tag{32}$$

These equations are the major results of this work. The modified impact factors are compared

to the experimental data as shown in Figures 4.4 through 4.6.

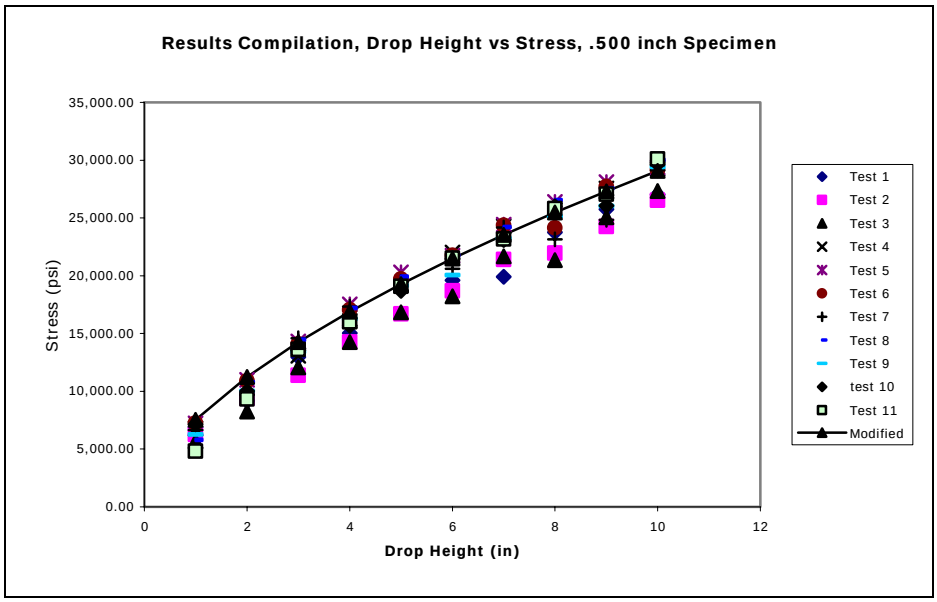

Figure 4.4 The stress from the modified impact factor compared to the experimental results for the .500 inch specimen.

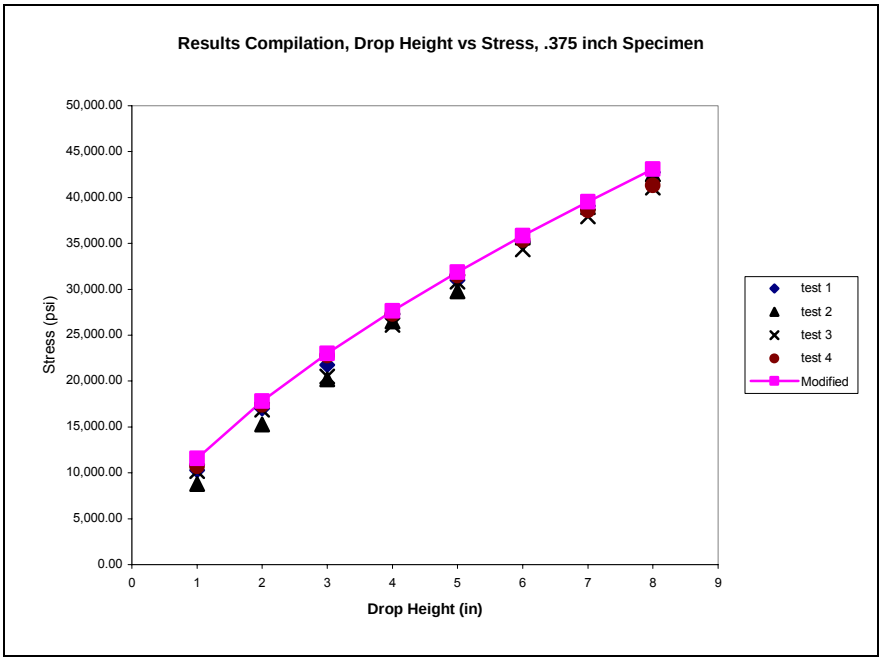

Figure 4.5 The stress from the modified impact factor compared to the experimental results for the .375 inch specimen.

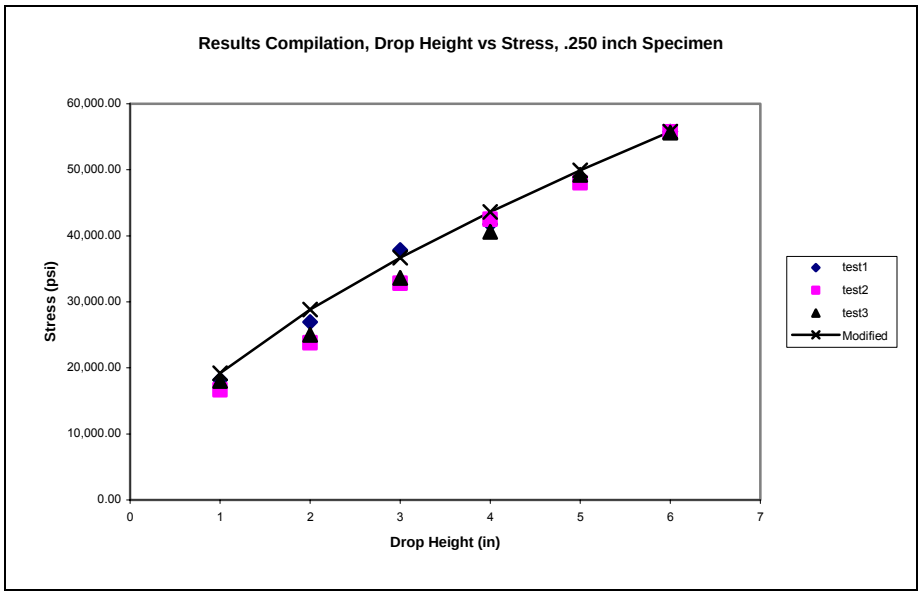

Figure 4.6 The stress from the modified impact factor compared to the experimental results for the .250 inch specimen.

CHAPTER 5

DISCUSSION

The experimental results clearly show that the work-energy method is overly conservative in its prediction of dynamic stress. This makes the work-energy impact equations quite ineffectual for design purposes. A part built utilizing these equations would be much larger and heavier than it really needs to be. As stated earlier, the goals of this project were to show that these equations are too conservative, modify them to be viable for design, and test the universality of these modifications.

The modified impact factors found account for the experimental data collected. The new equations can now be used to determine the approximate stress for the cantilevered beam from various heights as long as the stress remains in the elastic range. For the .500 inch specimen, a drop height of 36 inches results in a stress of 62 ksi. The bending modulus of yield of the original aircraft mount material, 7050-T7451, is 72 ksi. The bending modulus of yield of the example problem material, 2024-T3, is 52 ksi. The means the original aircraft part would not have yielded, but the example problem material would have. This is of course, an approximation. To fully utilize these new equations, appropriate load and safety factors must be incorporated. Also, any analysis of this type should be conservative in its initial assumptions. However, the main goal was accomplished. The impact equations are able to be used for design purposes.

The next portion of this project was to test the universality of the impact factor modification. The modified factors do not match from one geometry to another. The factors added to the equations are different as are the equation exponents. This implies the equations are only valid for the specific geometry and loading case for which they were formulated. They are not applicable to other impact problems at the moment. There are variables that have not

been investigated such as the impact of natural frequencies of the beam, solid viscosity, and deflected beam shape. These might lead to a more universal solution, instead of very specific modifications from empirical data.

There are areas of further study for this particular problem. The length of the cantilever can be changed to determine if the impact factors found hold or if they are not only a function of cross sectional geometry but cantilever length as well. Also, other materials such as steel can be tested. These changes would help to establish or eliminate possible variables to the modifications. On the theoretical side, variables such as natural frequencies can possibly be incorporated into the work-energy method to see if the empirical results can be accounted for. Once all of the variables are established it might be possible to determine what exactly is driving the modification to the impact factors and allow for a more universal application for design purposes. The finite element analysis that was performed shows that other geometries and loadings may be analyzed by simulation to verify the findings and expand them. The end result would be a straightforward, algebraic implementation which would be very useful to engineers in the design and analysis phases of a project.

APPENDIX A

TEST RESULTS

One test run for each specimen thickness is shown. The values from this data were used to formulate the equations in Chapter 3.

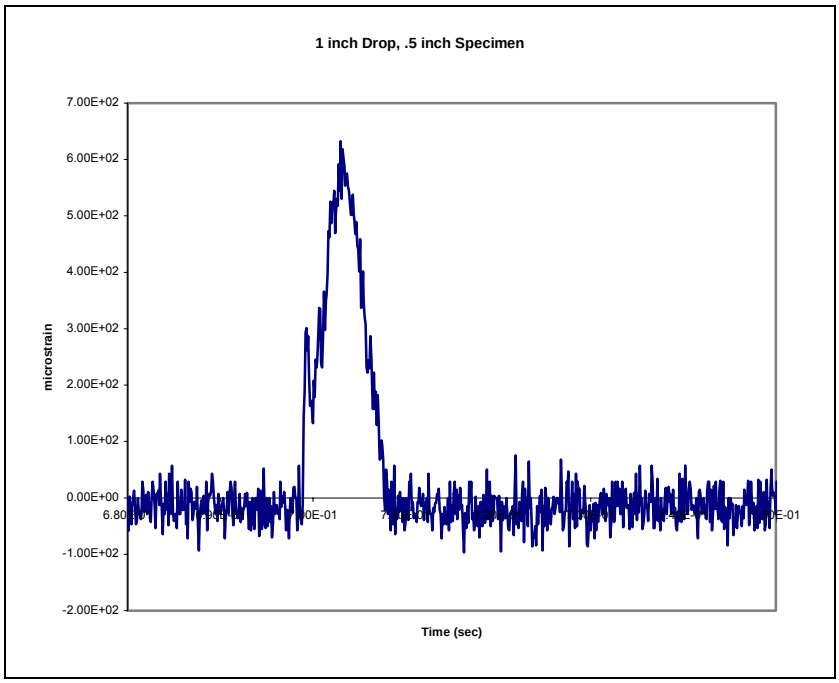

Figure A.1 One inch drop for the .5 inch specimen.

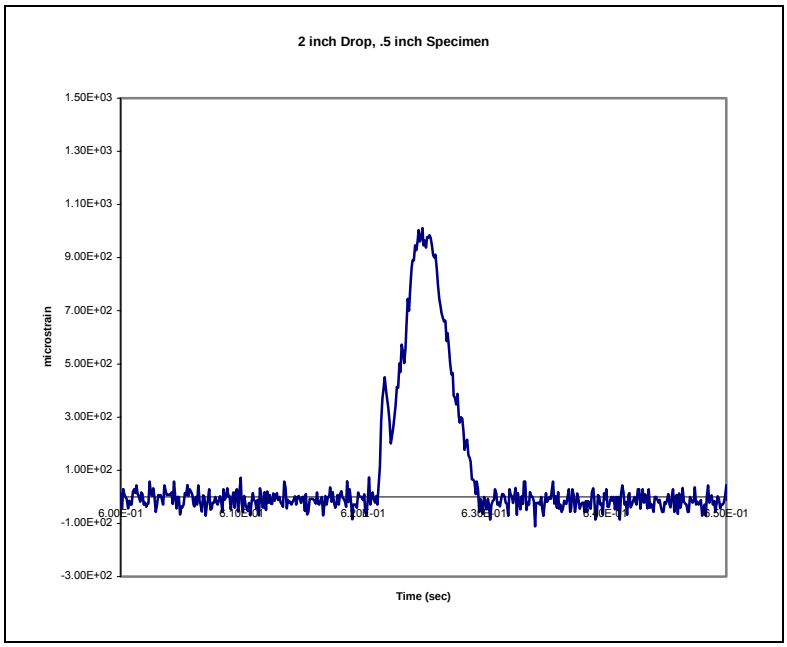

Figure A.2 Two inch drop for the .5 inch specimen.

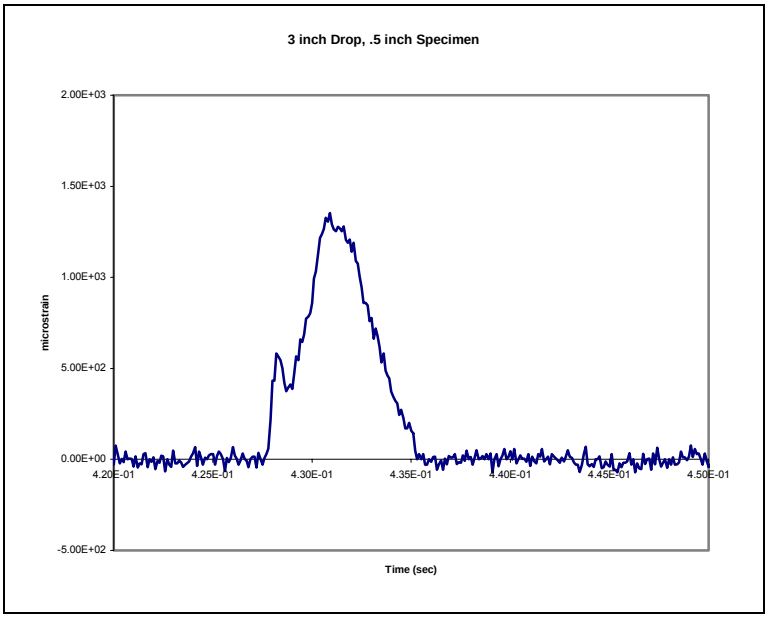

Figure A.3 Three inch drop for the .5 inch specimen.

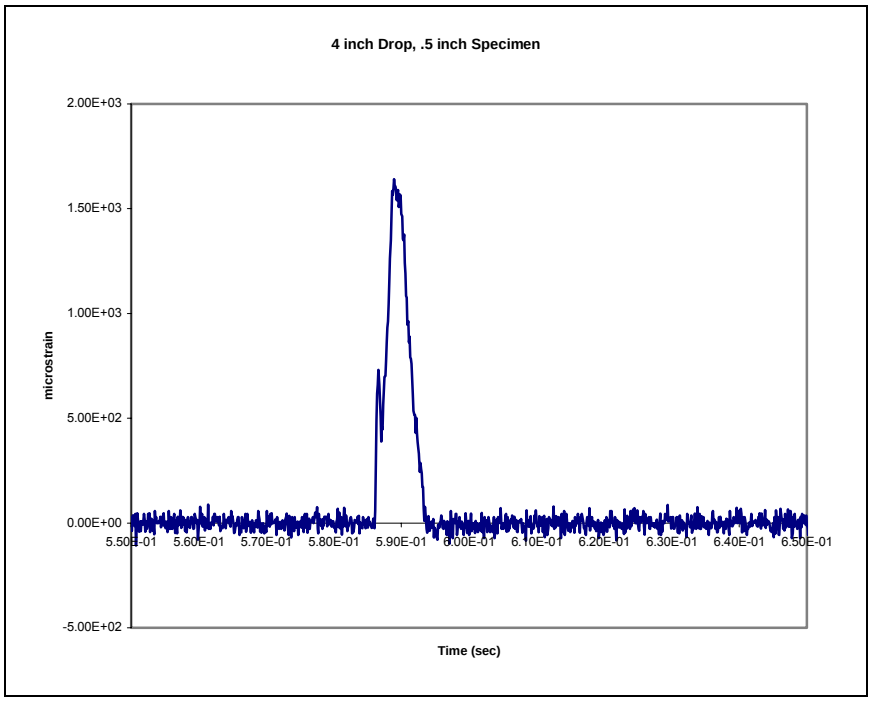

Figure A.4 Four inch drop for the .5 inch specimen.

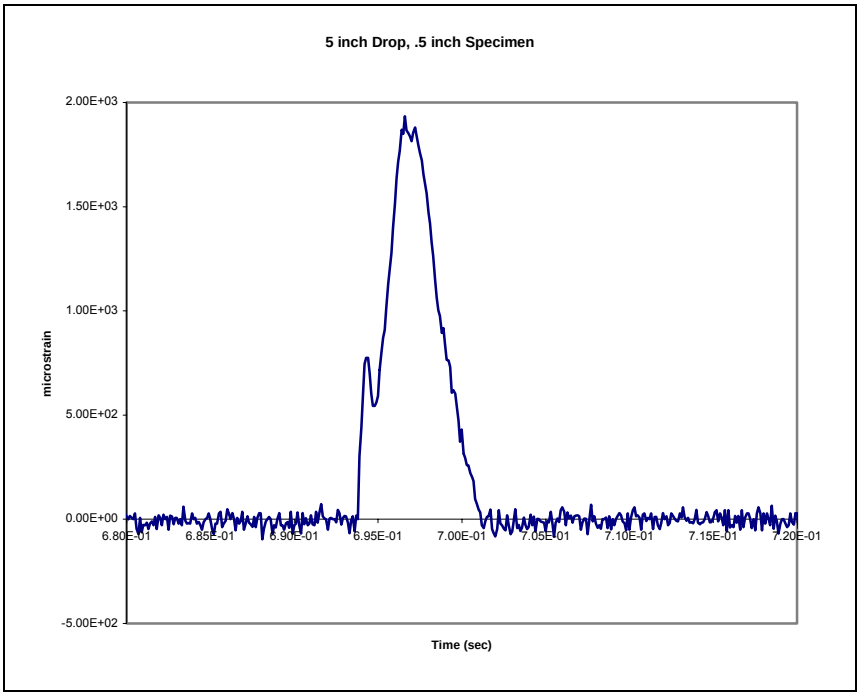

Figure A.5 Five inch drop for the .5 inch specimen.

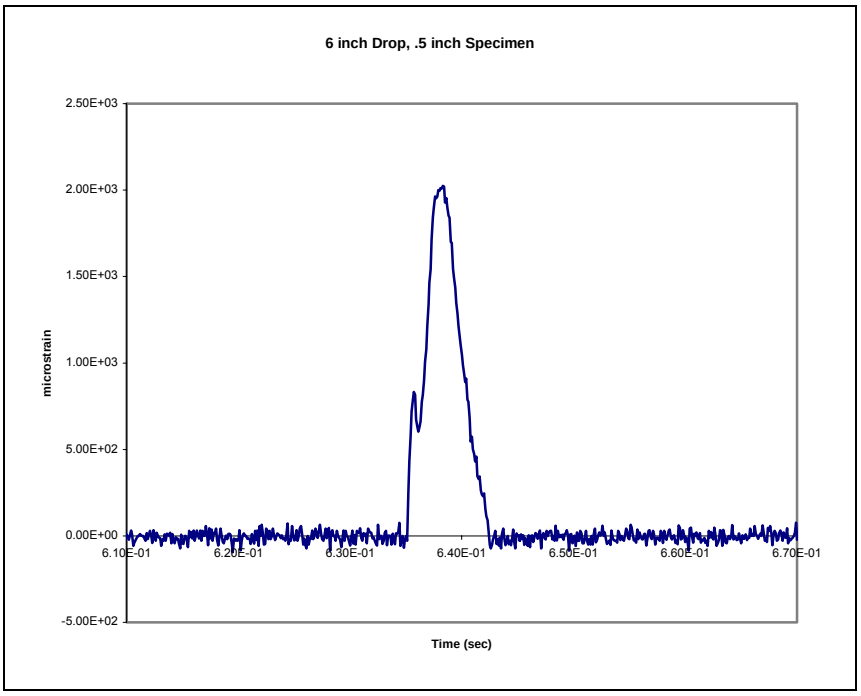

Figure A.6 Six inch drop for the .5 inch specimen.

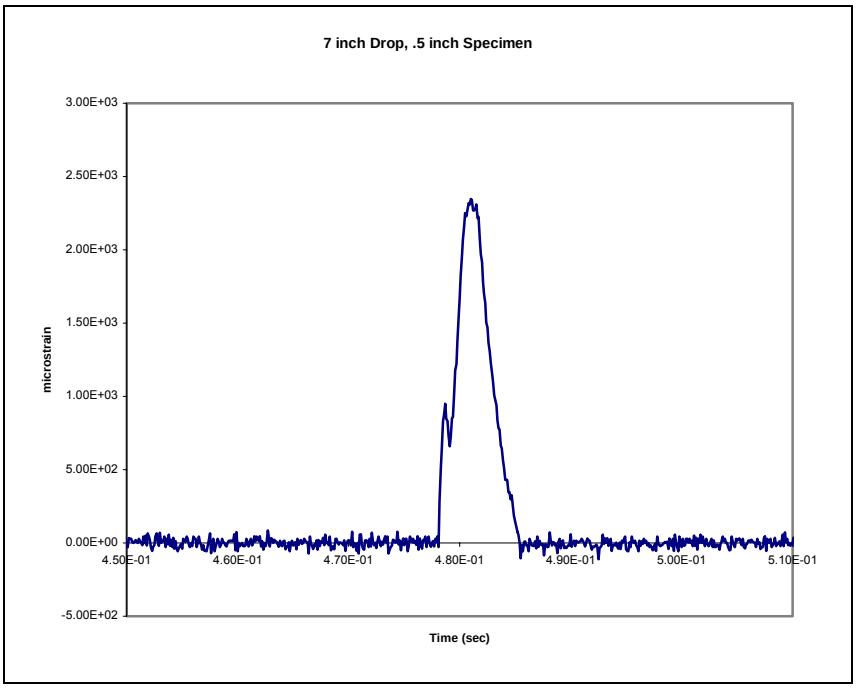

Figure A.7 Seven inch drop for the .5 inch specimen.

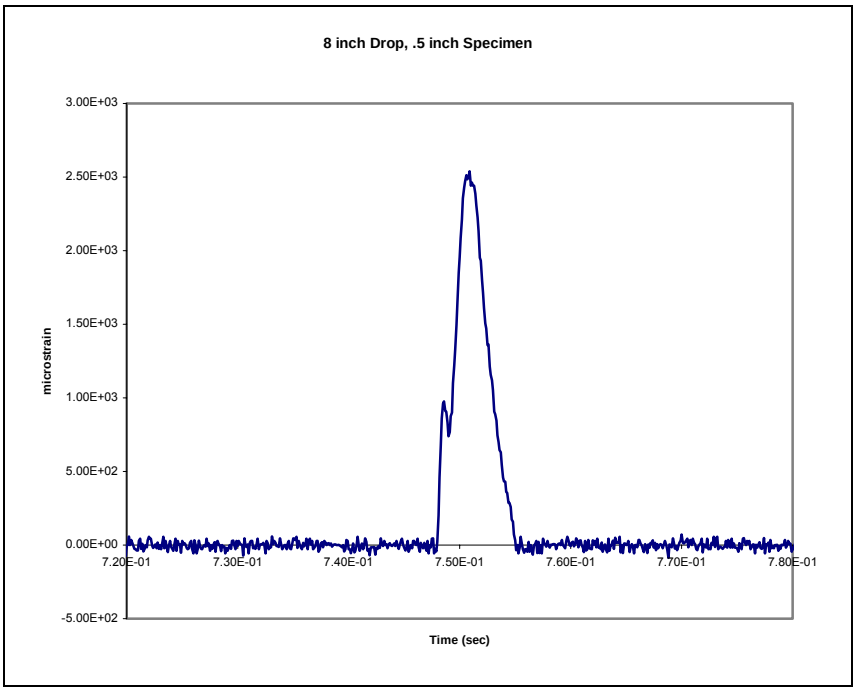

Figure A.8 Eight inch drop for the .5 inch specimen.

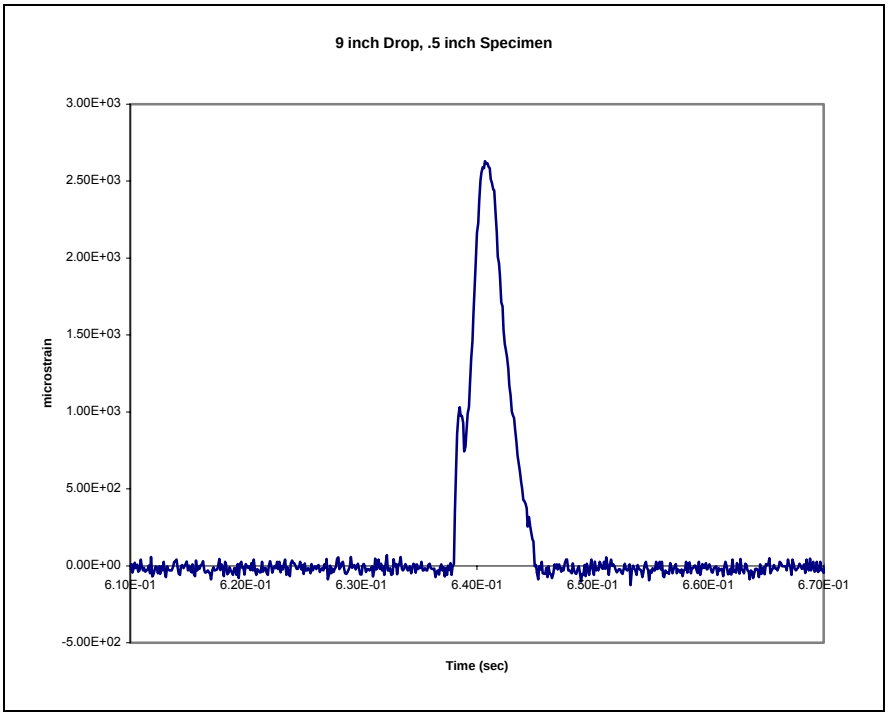

Figure A.9 Nine inch drop for the .5 inch specimen.

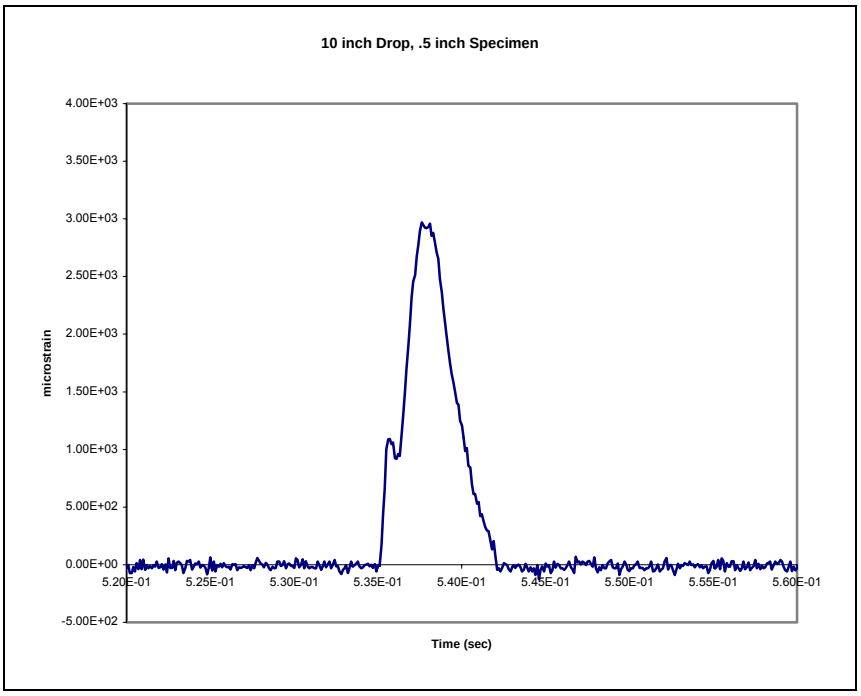

Figure A.10 Ten inch drop for the .5 inch specimen.

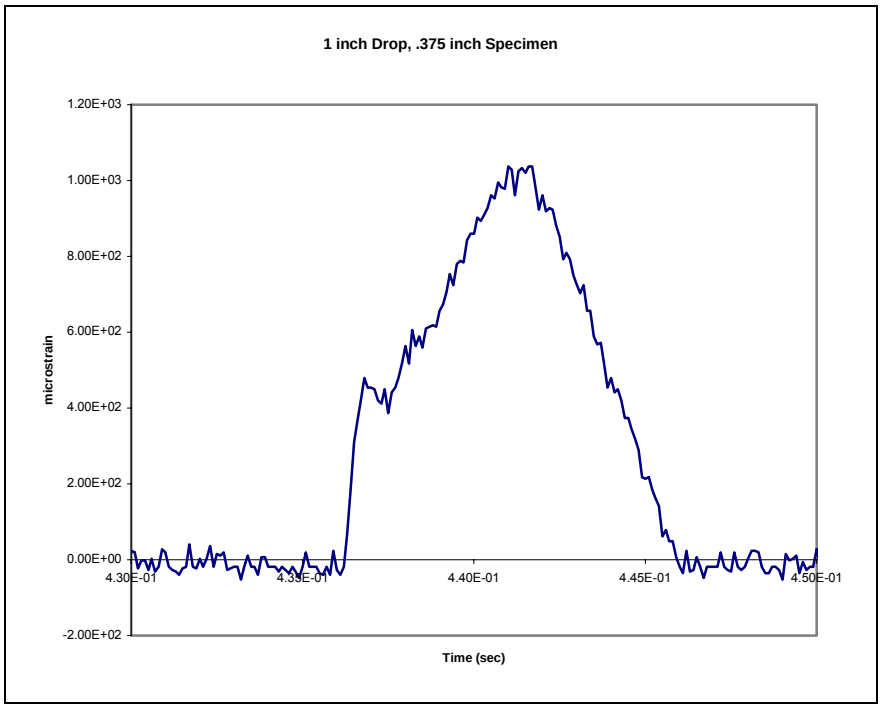

Figure A.11 One inch drop for the .375 inch specimen.

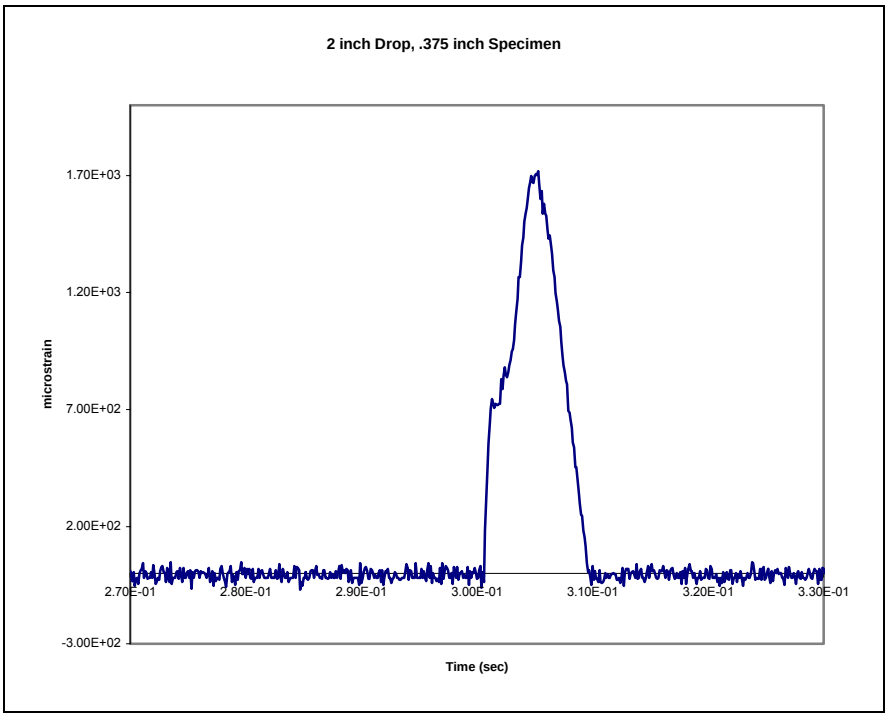

Figure A.12 Two inch drop for the .375 inch specimen.

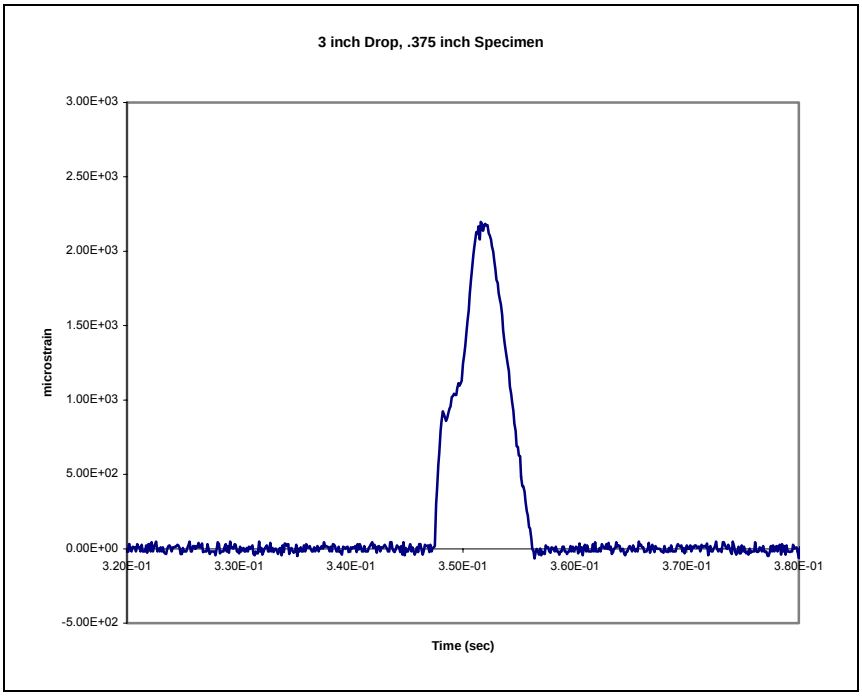

Figure A.13 Three inch drop for the .375 inch specimen.

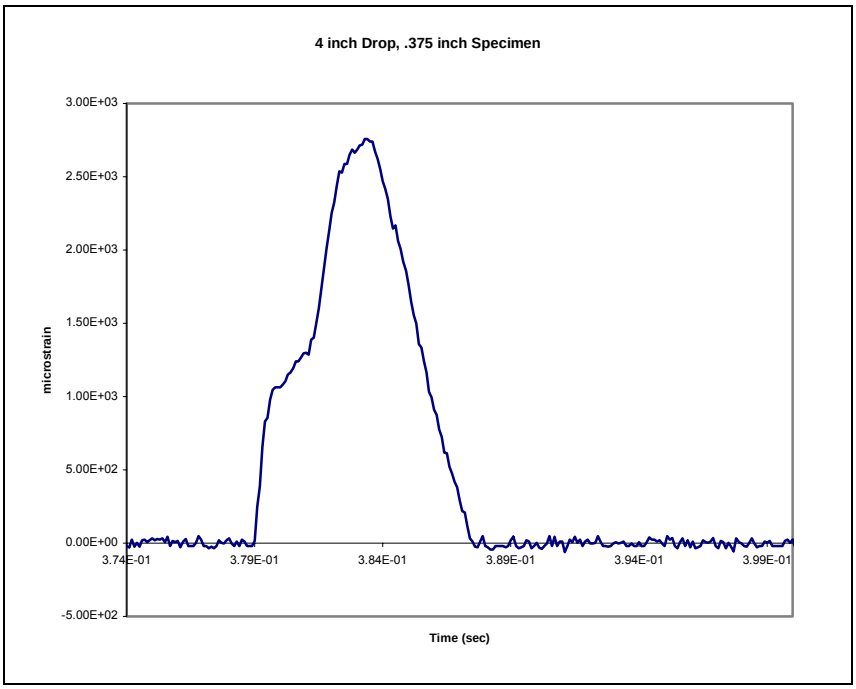

Figure A.14 Four inch drop for the .375 inch specimen.

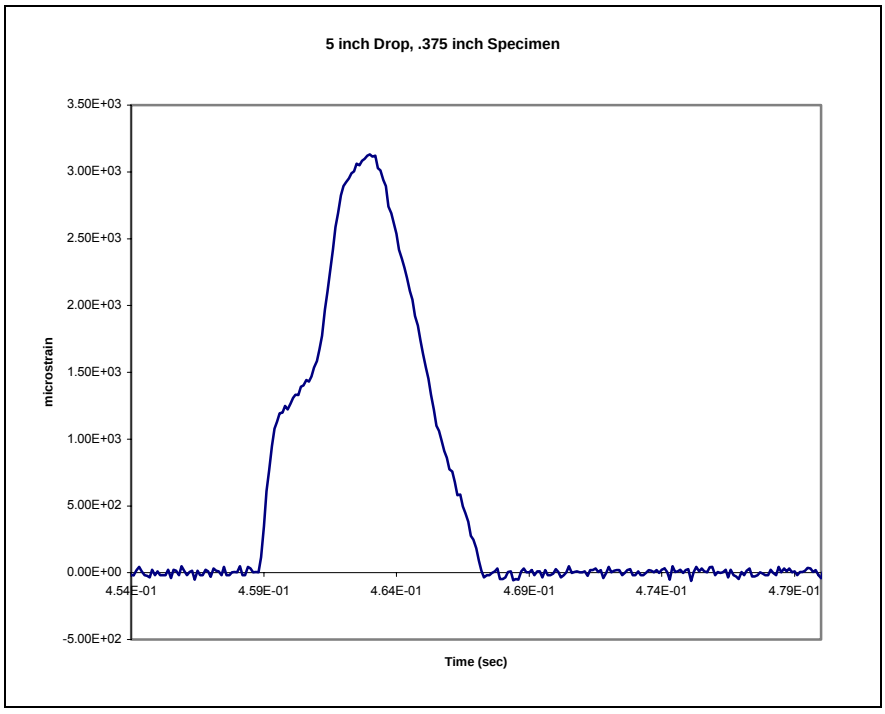

Figure A.15 Five inch drop for the .375 inch specimen.

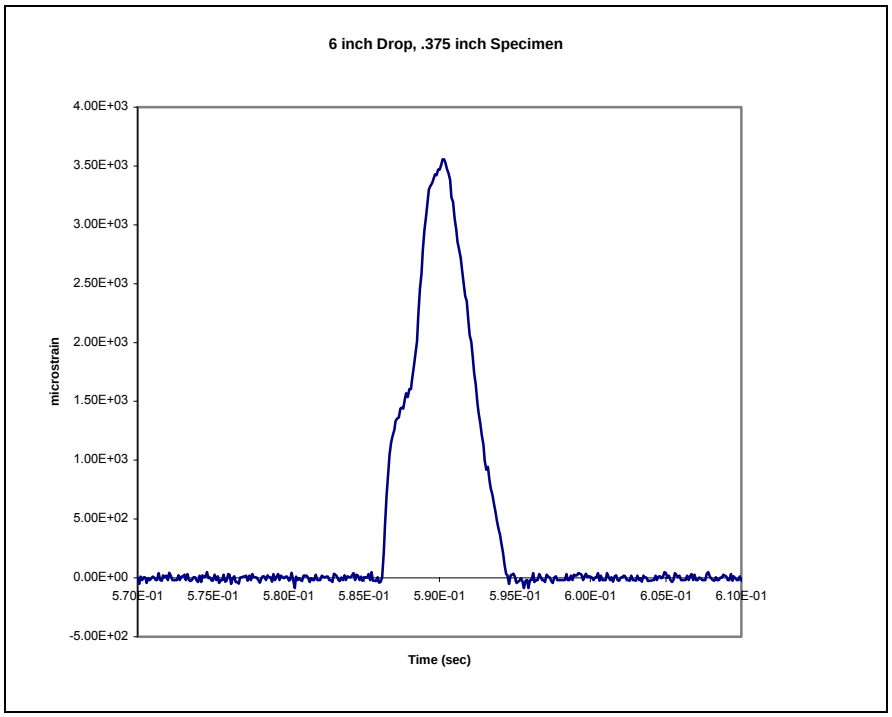

Figure A.16 Six inch drop for the .375 inch specimen.

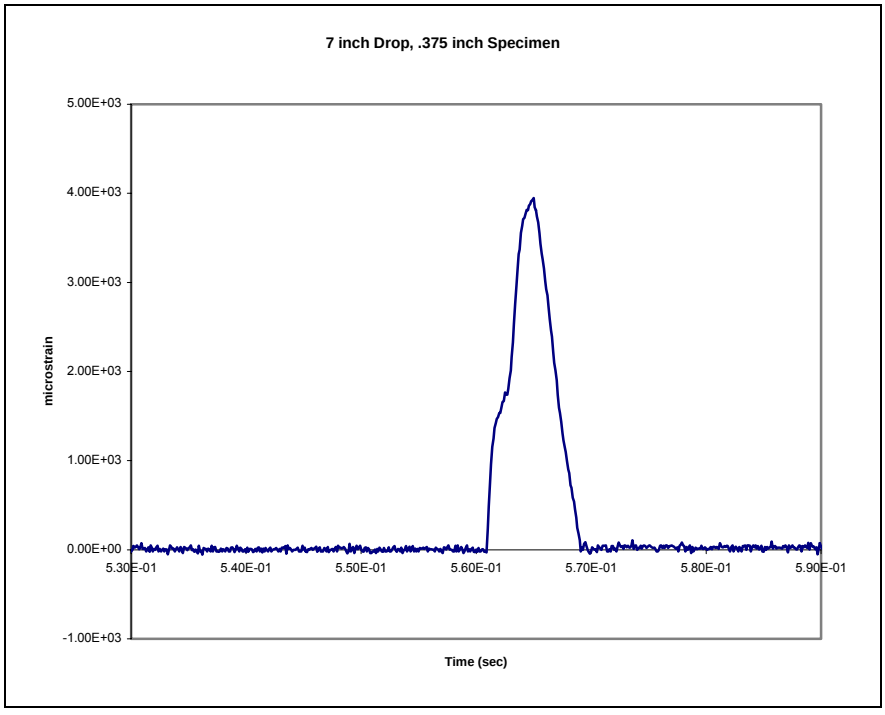

Figure A.17 Seven inch drop for the .375 inch specimen.

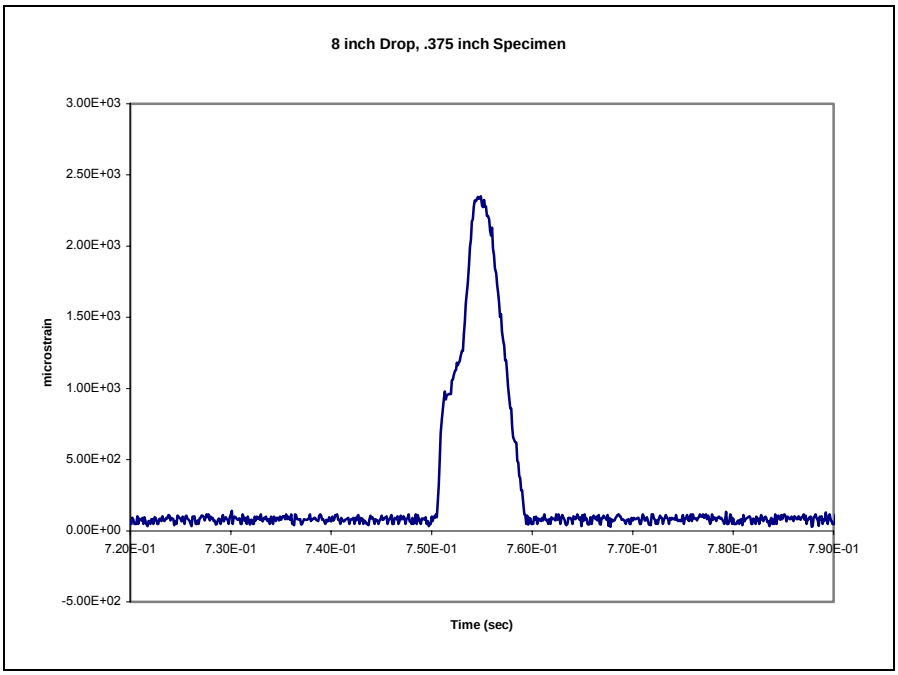

Figure A.18 Eight inch drop for the .375 inch specimen.

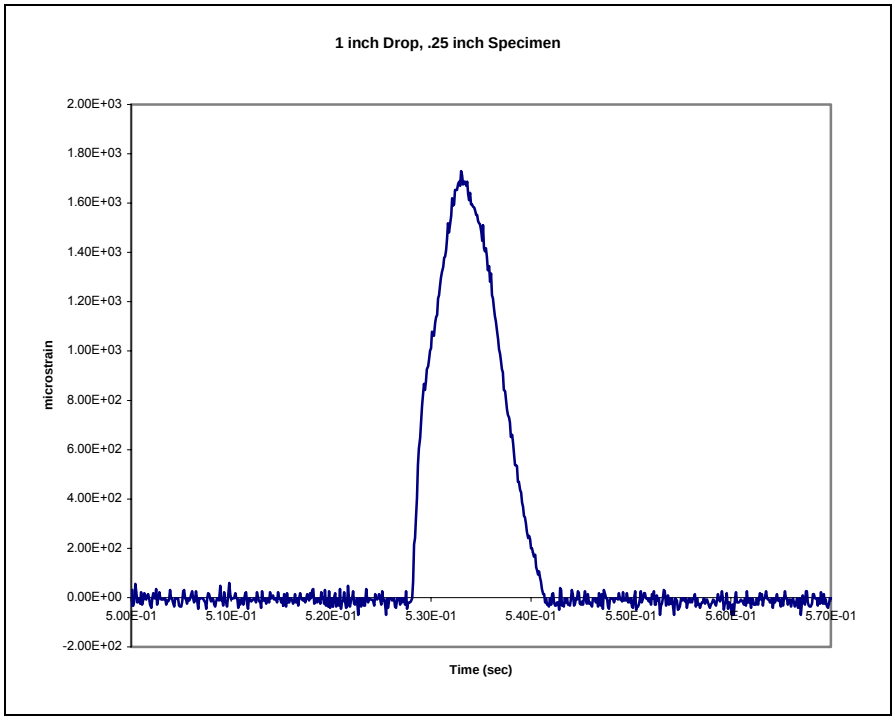

Figure A.19 One inch drop for the .25 inch specimen.

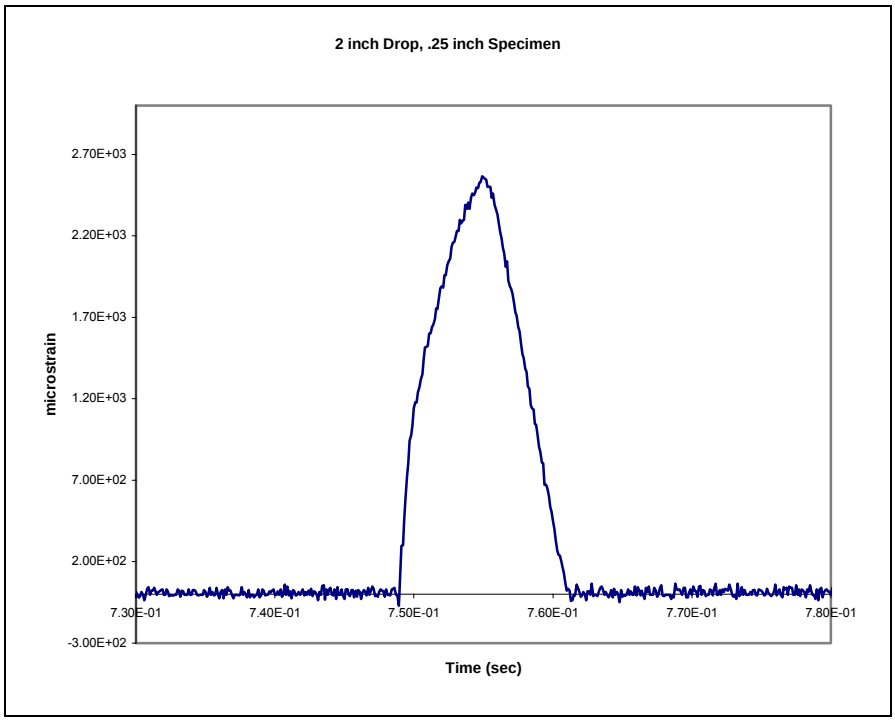

Figure A.20 Two inch drop for the .25 inch specimen.

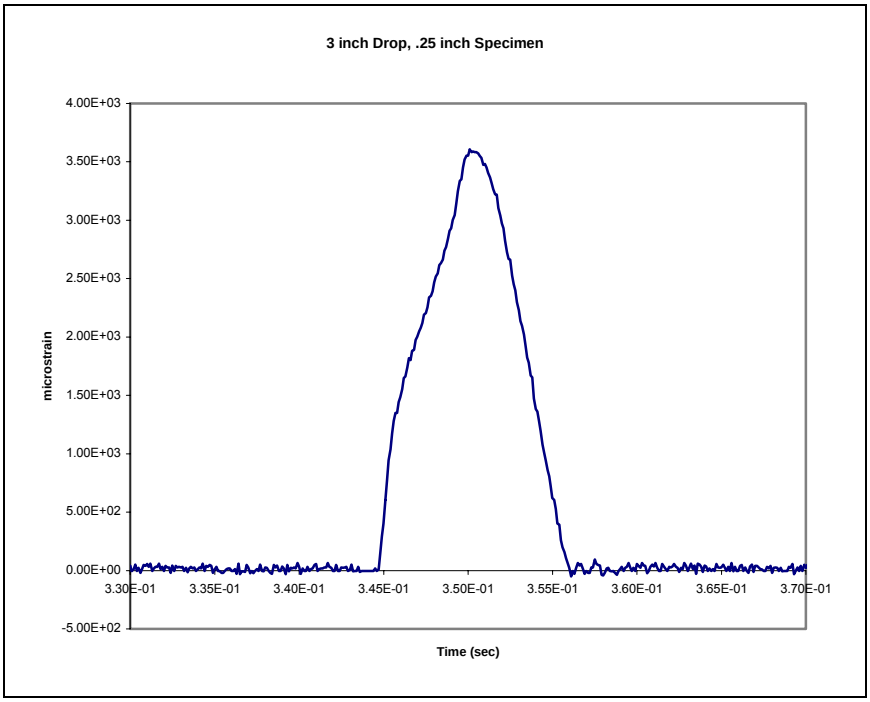

Figure A.21 Three inch drop for the .25 inch specimen.

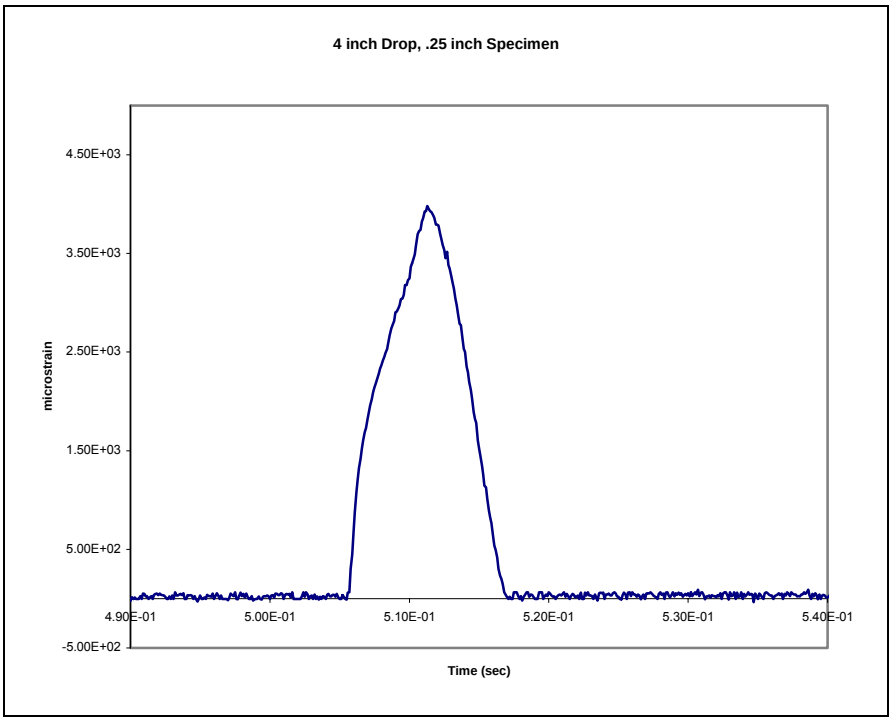

Figure A.22 Four inch drop for the .25 inch specimen.

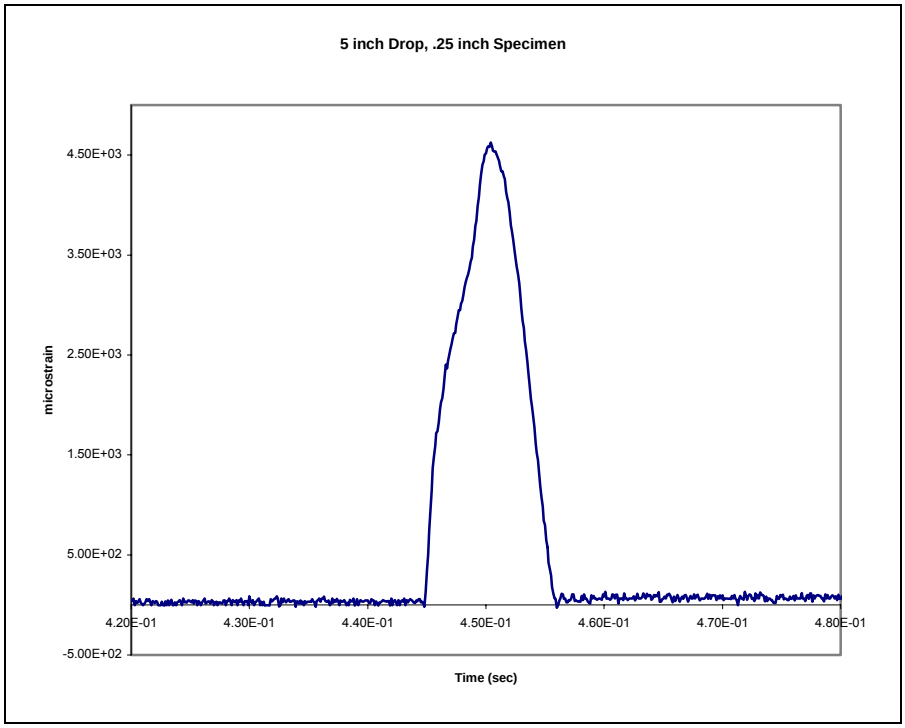

Figure A.23 Five inch drop for the .25 inch specimen.

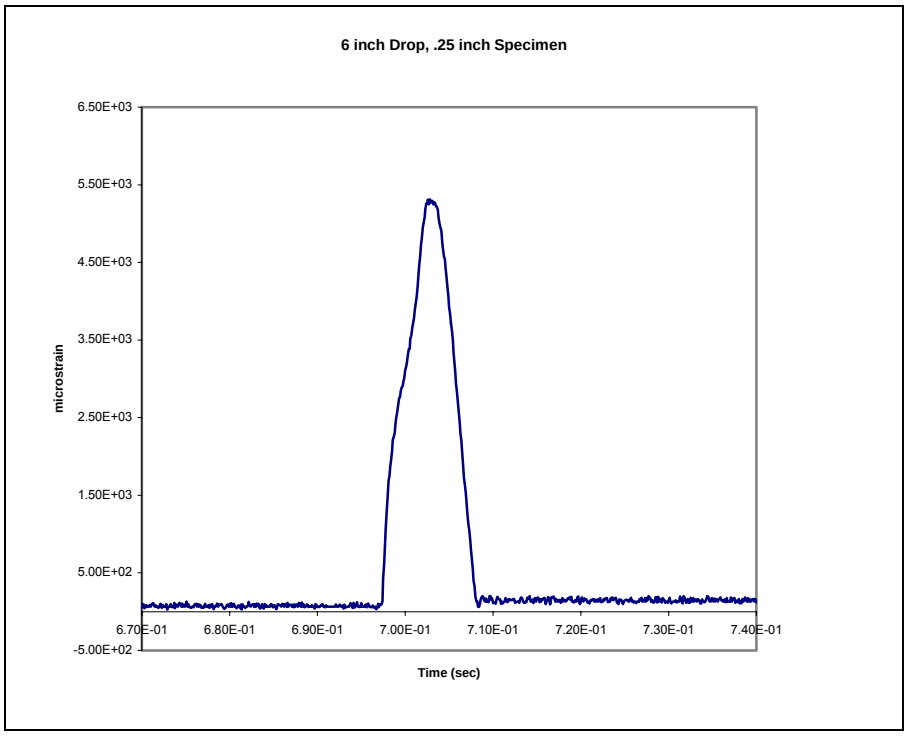

Figure A.24 Six inch drop for the .25 inch specimen.

REFERENCES

[1] T. Usuki, A. Maki, Behavior of beams under transverse impact according to higher-order beam theory, *International Journal of Solids and Structures* 40 (2003) 3737-3785.

[2] R. Chen, H. Zheng, S. Xue, H. Tang, Y. Wang, Analysis on transverse impact response of an unrestrained Timoshenko beam, *Applied Mathematics and Mechanics* 25 (2004) 1304-1313.

[3] Szuladzinski, G., Response of beams to shock loading; inelastic range, J*ournal of Engineering Mechanics* 133:3 (2007) 320-325.

[4] X.Q. Wang, R.M.C. So, K.T. Chan, Contributions of standing-wave components to dynamic stresses in a beam, *Journal of Sound and Vibration*310 (2008) 812-828.

[5] S. Suzuki, Measured dynamic-load factors of cantilever beams, frame structures and rings subjected to impulsive loads, *Experimental Mechanics* (1971) 76-81.

[6] Hibbeler, R.C. Mechanics of Materials. 6th ed. Upper Saddle River: Pearson Prentice Hall, 2005.

[7] Bruhn, E. Analysis and Design of Flight Vehicle Structures. Tri-State offset Company, 1973.

[8] Young, Warren, and Richard Budynas. Roark's Formulas for Stress Strain. 7th ed. New York: McGraw-Hill, 2002.

[9] Private Communication, Aditya Battin, 11/20/2009.

[10] Norton, Robert. Machine Design: An Integrated Approach. 3rd ed. Upper Saddle River: Pearson Prentice Hall, 2006.

[11] Ugural, Ansel and Saul Fenster. Advanced Strength and Applied Elasticity. 4th ed. Upper Saddle River: Prentice Hall, 2003.

[12] Timoshenko, S. Strength of Materials. 3rd ed. Malabar: Robert e. Krieger Publishing Company, 1984.

[13] Collins, J.A. Failure of Materials in Mechanical Design. New York: John Wiley and Sons, 1981.

[14] Riley, William, and Leroy Sturges. Engineering Mechanics: Dynamics. 2nd ed. New York: John Wiley and Sons, 1996.

[15] Craig, Roy, and Andrew Kurdila. Fundamentals of Structural Dynamics. 2nd ed. Hoboken: John Wiley and Sons, 2006.

BIOGRAPHICAL INFORMATION

Joshua Ballard earned his B.S.M.E. from the University of Texas at Arlington. He works in the aerospace industry, formerly designing helicopter modifications and currently designing composite rotor blades.